Appendix A.15:

Warrington St – CPT 44959

Table 1: Site Description for Warrington St (CPT 44959 – CC LIQ 10).

Attribute	Yes/No			Description/Date	Symbol in Figure 1
	10-m Buffer	20-m Buffer	50-m Buffer		
Near a body of surface water or other free face features?	No	No	No	The center of the site is 485 m from a creek bearing no name (~0.5 m high, NW-SE free face), 497 m away from Dudley Creek (~1.5 m high, NW-SE free-face), and 1700 m away from the Avon River (~3.0 m high, E-W free face).	NA
Lateral spreading observed during the CES?	No	No	No	Absence of ground cracks indicates no lateral spreading, as observed by the mapping team.[1]	NA
Nearby buildings or structures?	Yes	Yes	Yes	Building coverage of the 10-m, 20-m, and 50-m buffers is 36%, 47%, and 30%, respectively. Buildings are in all quadrants of the buffers.	White Fill + Brown Outline
Sloping land?	No	No	No	Flat land, residential area.	NA
Step changes in the ground surface?	No	No	No	NA	NA
Retaining walls?	No	No	No	NA	NA
Vegetation?	Yes	Yes	Yes	Trees and bushes cover 3% of the 10-m buffer, 18% of the 20-m buffer and 23% of the 50-m buffer. They are in the NW, SW, and SE quadrants of the 10-m buffer and in all quadrants of the 20-m and 50-m buffers.	White Fill + Green Outline
Manmade changes to the site between the LiDAR surveys?	No	No	No	NA	NA
Other important factors?	No	No	Yes	Moderate-motor-vehicle-volume roadway occupies 12% of the 50-m buffer and stretches throughout the S half of the buffer. Possible ditch (man-made or old stream channel) appears to be in the NW quadrant of the 50 m buffer.	Road: Gray Fill + Red Outline; Possible Ditch: Black Line

Note: Buffer is the area within a circle of a specified radius with CPT investigations done at its center (172.643107°, -43.508034°).

[1] Canterbury Geotechnical Database. (2012). "Observed Ground Crack Locations", Map Layer CGD0400 - 23 July 2012, retrieved July 09, 2018 from https://canterburygeotechnicaldatabase.projectorbit.com/

Figure 1: Site plan with areas where LiDAR survey data is considered.

Note 1: Two patches (outlined in red) in the free field were initially selected for settlement assessment as areas free of vegetation and structures. Further analyses such as proximity of a patch to a CPT, proximity of a patch to a property subjected to addition and/or demolition of a structure, front yard/backyard alterations (e.g., ploughing, rubble, scrap), spatial distribution of sediment ejecta, and density of LiDAR points for 2003 resulted in Patch A being selected for detailed settlement assessment and other patch being discarded in detailed settlement assessment. In addition, since significant amounts of ejecta were observed on roads in the CES, the entire portion of the road within the 50-m buffer was considered for settlement assessment. Roads as hard, relatively flat surfaces provide many ground-classified points. Therefore, it is very useful to compare settlement estimates on roads with settlement estimates for the unpaved patch.

Table 2: LiDAR flight error adjustments, global adjustments for the difference between average LiDAR point elevations and benchmark survey elevations, and vertical tectonic movement adjustments.

	Adjustments (mm)		
Earthquake Event(s)	LiDAR Flight Error	Global Offset[2]	Tectonic Vertical Movement
Sep-10	-100	-3	0
Feb-11	0	16	-75
Jun-11	0	38	-28
Dec-11	0	-65	-2
CES	-100	-14	-105
Post Sep 2010 LiDAR survey affected by ejecta?			No

Note: The negative sign indicates the subtraction from the ground surface subsidence, while the positive sign indicates the addition to the ground surface subsidence.

Table 3a: LiDAR Measurement Error for Patch A.

Surveys	Buffer	Area Averaged Difference Indicating Repeat Measurement Error (mm)	$\sigma^*_{\text{individual LiDAR points}}$ (mm)	%Reduction in σ due to Area Averaging of LiDAR Points
Post Feb 2011: Mar 2011 and May 2011	10-m	NA	59	[47,47]
	20-m	28		
	50-m	28		
Post Dec 2011: Feb 2012 and Oct 2015	10-m	NA	70	[9,9]
	20-m	6		
	50-m	6		

*Standard deviation.

[2] Russell, J., & van Ballegooy, S. (2015). *Canterbury Earthquake Sequence: Increased liquefaction vulnerability assessment methodology*. New Zealand: Tonkin & Taylor Ltd.

Table 3b: LiDAR Measurement Error for Road.

Surveys	Buffer	Area Averaged Difference Indicating Repeat Measurement Error (mm)	$\sigma^*_{\text{individual LiDAR points}}$ (mm)	%Reduction in σ due to Area Averaging of LiDAR Points
Post Feb 2011: Mar 2011 and May 2011	10-m	NA	59	[14,17]
	20-m	10		
	50-m	8		
Post Dec 2011: Feb 2012 and Oct 2015	10-m	NA	70	[67,89]
	20-m	47		
	50-m	62		

*Standard deviation.

Table 4a: Ground surface subsidence adjustments for Patch A due to LiDAR measurement error.

Earthquake Event(s)	$\sigma_{\text{pre-EQ LiDAR survey}}$ (mm)	$\sigma_{\text{post-EQ LiDAR survey}}$ (mm)	σ_{total} (mm)	Area Average Adjusted σ (mm)**
Sep-10	158	56	134	±64
Feb-11	56	59	59	±28
Jun-11	59	61	62	±30
Dec-11	61	70	87	±41
CES	158	70	124	±59

**Based on the highest %Reduction in Table 3a.

Table 4b: Ground surface subsidence adjustments for Road due to LiDAR measurement error.

Earthquake Event(s)	$\sigma_{\text{pre-EQ LiDAR survey}}$ (mm)	$\sigma_{\text{post-EQ LiDAR survey}}$ (mm)	σ_{total} (mm)	Area Average Adjusted σ (mm)**
Sep-10	158	56	134	±119
Feb-11	56	59	59	±52
Jun-11	59	61	62	±55
Dec-11	61	70	87	±77
CES	158	70	124	±110

**Based on the highest %Reduction in Table 3b.

Table 5a: Raw liquefaction-related ground surface subsidence for Patch A using original LiDAR points.

	Average Ground Surface Subsidence (mm)		
Earthquake Event(s)	10-m Buffer	20-m Buffer	50-m Buffer
Sep-10	135	135	135
Feb-11	104	104	104
Jun-11	5	5	5
Dec-11	62	62	62
CES	306	306	306

Table 5b: Raw liquefaction-related ground surface subsidence for Road using original LiDAR points.

	Average Ground Surface Subsidence (mm)		
Earthquake Event(s)	10-m Buffer	20-m Buffer	50-m Buffer
Sep-10	NA	85	62
Feb-11	NA	144	138
Jun-11	NA	27	30
Dec-11	NA	51	50
CES	NA	308	280

Table 6a: Corrected liquefaction-related ground surface subsidence for Patch A using original LiDAR points with the calculated adjustments in Table 2.

	Average Calculated Ground Surface Subsidence (mm)		
Earthquake Event(s)	10-m Buffer	20-m Buffer	50-m Buffer
Sep-10	32±75	32±75	32±75
Feb-11	45±25	45±25	45±25
Jun-11	15±25	15±25	15±25
Dec-11	-5±50	-5±50	-5±50
CES	87±50	87±50	87±50

Notes: Plus/minus values are same as those in Table 4a, but rounded to the nearest 25; Positive overall values indicate ground surface subsidence, while negative overall values indicate ground surface uplift.

Table 6b: Corrected liquefaction-related ground surface subsidence for Road using original LiDAR points with the calculated adjustments in Table 2.

	Average Calculated Ground Surface Subsidence (mm)		
Earthquake Event(s)	10-m Buffer	20-m Buffer	50-m Buffer
Sep-10	NA	-18±125	-41±125
Feb-11	NA	85±50	79±50
Jun-11	NA	37±50	40±50
Dec-11	NA	-16±75	-17±75
CES	NA	89±100	61±100

Notes: Plus/minus values are same as those in Table 4b, but rounded to the nearest 25; Positive overall values indicate ground surface subsidence, while negative overall values indicate ground surface uplift.

Table 7a: Corrected liquefaction-related ground surface subsidence for Patch A using LiDAR DEMs.

	Estimated Ground Surface Subsidence (mm)								
	10-m Buffer			20-m Buffer			50-m Buffer		
Earthquake Event(s)	16th %ile	50th %ile	84th %ile	16th %ile	50th %ile	84th %ile	16th %ile	50th %ile	84th %ile
Sep-10	<50	50	50	<50	50	50	<50	50	50
Feb-11	<50	50	50	<50	50	50	<50	50	50
Jun-11	<50	50	50	<50	50	50	<50	50	50
Dec-11	<50	50	50	<50	50	50	<50	50	50
CES	100	150	150	100	150	150	100	150	150

Note: These percentiles are not the exact statistical measures; they indicate the spatial variability of ground surface subsidence.

Table 7b: Corrected liquefaction-related ground surface subsidence for Road using LiDAR DEMs.

	Estimated Ground Surface Subsidence (mm)								
	10-m Buffer			20-m Buffer			50-m Buffer		
Earthquake Event(s)	16th %ile	50th %ile	84th %ile	16th %ile	50th %ile	84th %ile	16th %ile	50th %ile	84th %ile
Sep-10	NA	NA	NA	<50	<50	50	<50	<50	50
Feb-11	NA	NA	NA	<50	50	50	<50	50	150
Jun-11	NA	NA	NA	<50	50	50	<50	50	50
Dec-11	NA	NA	NA	<50	50	50	<50	50	50
CES	NA	NA	NA	100	150	150	100	150	250

Note: These percentiles are not the exact statistical measures; they indicate the spatial variability of ground surface subsidence.

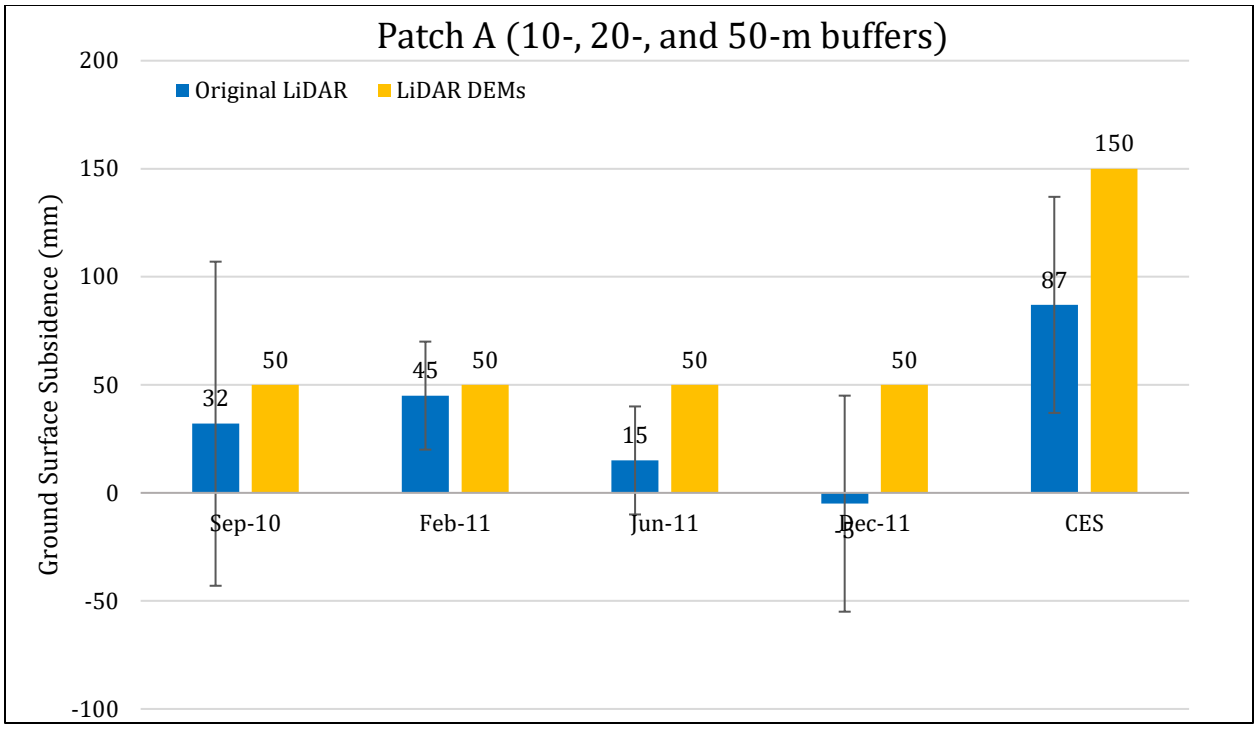

Figure 2: Comparison between ground surface subsidence determined from original LiDAR survey points and ground surface subsidence (50th %ile) estimated using LiDAR DEMs for the 20-m buffer.

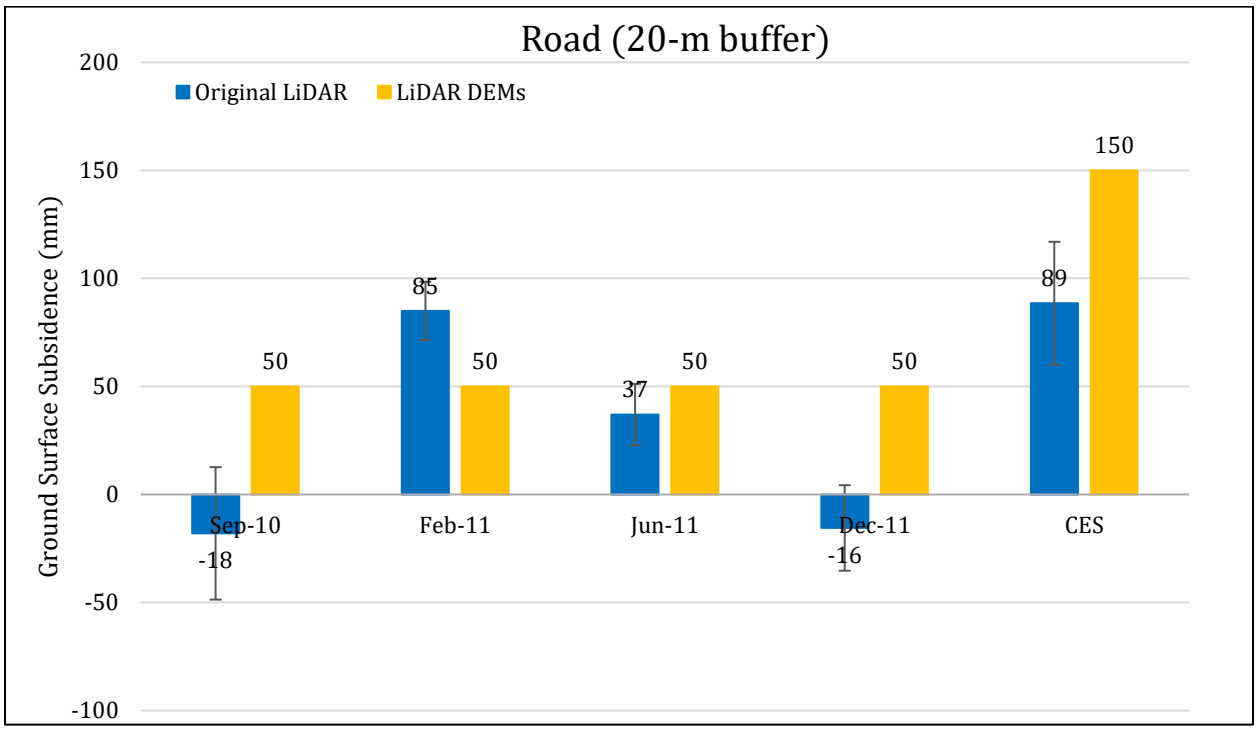

Figure 3: Comparison between ground surface subsidence determined from original LiDAR survey points and ground surface subsidence (50th %ile) estimated using LiDAR DEMs for Road for the 20-m buffer.

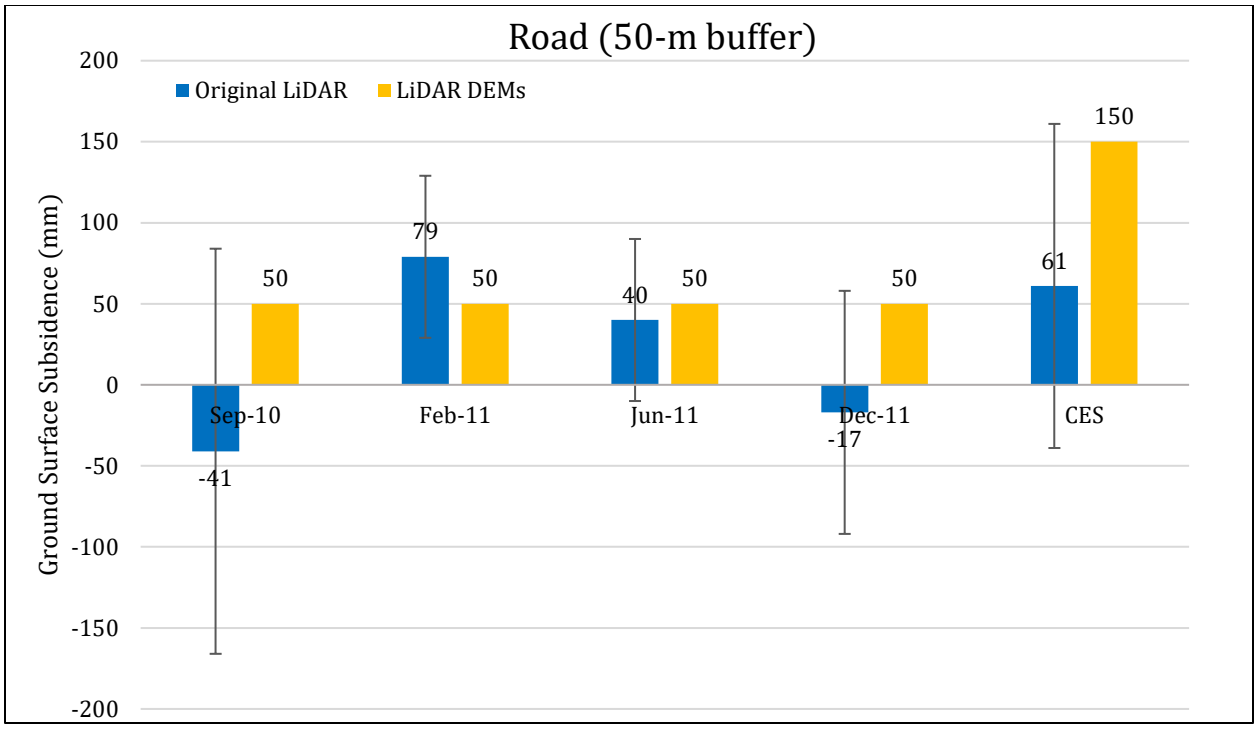

Figure 4: Comparison between ground surface subsidence determined from original LiDAR survey points and ground surface subsidence (50th %ile) estimated using LiDAR DEMs for Road for the 50-m buffer.

Note 2: The ground surface subsidence values determined from original LiDAR survey points are generally similar to the ground surface subsidence values estimated using LiDAR DEMs for all earthquake events.

Table 8a: Ejecta-Induced settlement for the top 20 m of the soil profile for Patch A within the 50-m buffer for the 50th %ile PGA, P_L=50%, and C_{FC}=0.13 using BI-2014, ZRB-2002, and I_c cutoff of 2.6.

Earthquake Event(s)	M_W	PGA (g)	Depth to Groundwater (m)	S_T(mm)	S_{V1D} (mm)	$S_{E,L}$ (mm)
Sep-10	7.1	0.20	1.5	32±75	10±20	22±78
Feb-11	6.2	0.36	1.5	45±25	46±50	-1±56
Jun-11	6.2	0.20	0.7	15±25	17±25	-2±35
Dec-11	6.1	0.23	0.8	-5±50	23±50	-28±71

Notes: S_T = Total settlement (Table 6); S_{V1D} = Average vertical settlement due to volumetric compression using Boulanger and Idriss (2014) (BI-2014) and Zhang et al. (2002) (ZRB-2002) procedures and de Greef and Lengkeek (2018) thin-layer correction; $S_{E,L}$ = Ejecta-induced settlement as the difference between the LiDAR-based S_T and S_{V1D}; NA = Not available.

Table 8b: Ejecta-Induced settlement for the top 20 m of the soil profile for Road within the 20-m buffer for the 50th %ile PGA, P_L=50%, and C_{FC}=0.13 using BI-2014, ZRB-2002, and I_C cutoff of 2.6.

Earthquake Event(s)	M_W	PGA (g)	Depth to Groundwater (m)	S_T(mm)	S_{V1D} (mm)	$S_{E,L}$ (mm)
Sep-10	7.1	0.20	1.5	-18±125	9±20	-27±127
Feb-11	6.2	0.36	1.5	85±50	30±50	55±71
Jun-11	6.2	0.20	0.7	37±50	15±25	22±56
Dec-11	6.1	0.23	0.8	-16±75	20±50	-36±90

Notes: S_T = Total settlement (Table 6); S_{V1D} = Average vertical settlement due to volumetric compression using Boulanger and Idriss (2014) (BI-2014) and Zhang et al. (2002) (ZRB-2002) procedures and de Greef and Lengkeek (2018) thin-layer correction; $S_{E,L}$ = Ejecta-induced settlement as the difference between the LiDAR-based S_T and S_{V1D}; NA = Not available.

Table 8c: Ejecta-Induced settlement for the top 20 m of the soil profile for Road within the 50-m buffer for the 50th %ile PGA, P_L=50%, and C_{FC}=0.13 using BI-2014, ZRB-2002, and I_C cutoff of 2.6.

Earthquake Event(s)	M_W	PGA (g)	Depth to Groundwater (m)	S_T(mm)	S_{V1D} (mm)	$S_{E,L}$ (mm)
Sep-10	7.1	0.20	1.5	-41±125	9±20	-50±127
Feb-11	6.2	0.36	1.5	79±50	30±50	49±71
Jun-11	6.2	0.20	0.7	40±50	15±25	25±56
Dec-11	6.1	0.23	0.8	-17±75	20±50	-37±90

Notes: S_T = Total settlement (Table 6); S_{V1D} = Average vertical settlement due to volumetric compression using Boulanger and Idriss (2014) (BI-2014) and Zhang et al. (2002) (ZRB-2002) procedures and de Greef and Lengkeek (2018) thin-layer correction; $S_{E,L}$ = Ejecta-induced settlement as the difference between the LiDAR-based S_T and S_{V1D}; NA = Not available.

Note 3: The uncertainty for volumetric settlement was derived based on the sensitivity of volumetric settlement to PGA, C_{FC}, and P_L for each earthquake event for VsVp 57203 *Shirley Intermediate School* and CC LIQ 1 – CPT 5586 – *Vivian St* sites. Taking the 50th percentile as the baseline case, the minimum and maximum values corresponding to the difference between the 25th percentile and the 50th percentile and the 75th percentile and the 50th percentile were determined. The arithmetic mean of the range of the minimum and maximum difference was evaluated for each patch at the two sites. The maximum arithmetic mean for each earthquake event was rounded to the nearest five and used as the uncertainty value. Accordingly, the 1-D volumetric settlement uncertainties of ±20, ±50, ±25, and ±50 mm for the Sep-10, Feb-11, Jun-11, and Dec-11 earthquake events, respectively, were used for all sites in this study.

Table 9a: Coverage area and height of ejecta estimates for Patch A using aerial and/or ground photographs and engineering judgement.

Earthquake Event	$H_{E,thin}$ (mm)	$A_{E,thin}$ (m^2)	$H_{E,thick}$ (mm)	$A_{E,thick}$ (m^2)	A_T (m^2)
Sep-10	0	0	0	0	37.7
Feb-11	10-20	13.2	50-70	21.6	37.7
Jun-11	NA	NA	NA	NA	37.7
Dec-11	0	0	0	0	37.7

Note: NA = Not available as no aerial and/or ground photograph was acquired for the site; $A_{E,thick/thin}$ = Coverage area of thick/thin ejecta layers; $H_{E,thick/thin}$ = Lower-upper estimate of height of thick/thin ejecta layers; $H_{E,prism/pyr}$ = Lower-upper estimate of ejecta height near the curb based on 2-4% cross slope of normal crown; $V_{E,prism+pyr}$ = Lower-upper estimate of total volume of prismatic- and pyramidal-shape ejecta; Thin and thick layers correspond to light gray and dark gray colors of ejecta observed in aerial photographs.

Table 9b: Coverage area and height of ejecta estimates for Road within the 50-m buffer using aerial and/or ground photographs and engineering judgement.

Earthquake Event	$H_{E,thin}$ (mm)	$A_{E,thin}$ (m^2)	$H_{E,prism}$ (mm)	$V_{E,prism}$ (m^3)	$H_{E,cc}$ (mm)	$V_{E,cc}$ (m^3)	A_T (m^2)
Sep-10	2-4	749	11-67	0.919-1.84	0	0	1222*
Feb-11	2-4	947	7-200	2.47-5.13	393-866	11.1	1166*
Jun-11	2-4	1070	9-80	0.937-1.87	681-894	4.45	1165*
Dec-11	3-6	46.7	10-56	0.082-0.164	0	0	1271

Note: $A_{E,thick/thin}$ = Coverage area of thick/thin ejecta layers; $H_{E,thick/thin}$ = Lower-upper estimate of height of thick/thin ejecta layers; $H_{E,prism}$ = Lower-upper estimate of ejecta height near the curb based on 2-4% cross slope of normal crown; $V_{E,prism}$ = Lower-upper estimate of total volume of prismatic-shape ejecta; Thin and thick layers correspond to light gray and dark gray colors of ejecta observed in aerial photographs; $V_{E,cc}$ = Volume of conically shaped ejecta pile components; $H_{E,cc}$ = Lower-upper estimate of height of conically shaped ejecta pile components (based on the repose angle of 30°); A_T= Total assessment area of a buffer being considered; * indicates reduction in A_T due to the presence of objects within the assessment area.

Note 4: The values in Table 9 correspond to the coverage area of ejecta outlined in aerial photographs (Figures 62 through 66) and the lower and upper estimates of ejecta height based on geometry, EQC LDAT property inspection notes (Figure 67) and reports from Sep 2013. The ejecta-induced settlement using photographs and engineering judgment, $S_{E,P}$, is estimated as

$$S_{E,P} = \frac{\sum_{i=1}^{a} A_{E,thick,i} * H_{E,thick,i} + \sum_{j=1}^{b} A_{E,thin,j} * H_{E,thin,j} + \frac{1}{2}\sum_{n=1}^{f} W_{E,prism,n} * H_{E,prism,n} * L_{E,prism,n}}{A_T} + \frac{\frac{1}{3}\sum_{k=1}^{c} A_{E,pile,k} * R_{E,pile,k} * tan30°}{A_T} = \frac{\sum_{i=1}^{a} V_{E,thick,i} + \sum_{j=1}^{b} V_{E,thin,j} + \sum_{n=1}^{f} V_{E,prism,n} + \sum_{k=1}^{c} V_{E,conical\ component,k}}{A_T}$$

where

- $A_{E,thick,i}$ and $H_{E,thick,i}$ are the area and the height of a thick ejecta layer, respectively;
- $A_{E,thin,j}$ and $H_{E,thin,j}$ are the area and the height of a thin ejecta layer, respectively;
- $W_{E,prism,n}$ and $L_{E,prism,n}$ are the width and the length of the coverage area of a prismatically shaped ejecta layer, respectively, and $H_{E,prism,n}$ is the height of a prism-like ejecta layer;
- $A_{E,pile,k}$ and $R_{E,pile,k}$ are the area and the radius of an ejecta pile component, respectively, shaped as a cone with the repose angle of 30°;
- A_T is the total assessment area for a buffer being considered (Figure 1).

Table 10: Ejecta-induced settlement estimates based on aerial and/or ground photographs.

Earthquake Event	Patch A (10-, 20-, and 50-m buffers)		Road (50-m buffer)	
	$S_{E,P,lower}$ (mm)	$S_{E,P,upper}$ (mm)	$S_{E,P,lower}$ (mm)	$S_{E,P,upper}$ (mm)
Sep-10	0	0	2	4
Feb-11	32	47	13	17
Jun-11	NA	NA	7	9
Dec-11	0	0	≈0	≈0

Note: $S_{E,P,lower}$ and $S_{E,P,upper}$ correspond to lower and upper estimates of $S_{E,P}$, respectively; NA = Not available due to the lack of physical evidence.

Table 11: Best final estimates of ejecta-induced settlement.

Earthquake Event	Patch A (10-, 20-, and 50-m buffers)			Road (50-m buffer)		
	$S_{E,L}$ (mm)	$S_{E,P}$ (mm)	$S_{E,final}$ (mm)	$S_{E,L}$ (mm)	$S_{E,P}$ (mm)	$S_{E,final}$ (mm)
Sep-10	22±78	0	0	-50±127	3±1	5±5
Feb-11	-1±56	39±8	40±10	49±71	15±2	25±25
Jun-11	-2±35	NA	NA	25±56	8±1	15±20
Dec-11	-28±71	0	0	-37±90	≈0	<5

Notes: $S_{E,L}$ = Ejecta-induced settlement based on LiDAR data reported in Table 8; $S_{E,P}$ = Median ejecta-induced settlement for the range of values reported in Table 10; $S_{E,final}$ = Best final estimate of ejecta-induced settlement rounded to the nearest 5; Final plus/minus values are also rounded to the nearest 5; NA = Not available due to the lack of physical evidence.

Note 5:

- $S_{E,final}$ for Patch A for the Sep-10, Feb-11, and Dec-11 EQs is based solely on $S_{E,P}$. For the Jun-11 EQ, the ejecta-induced settlement within Patch A is not available due to the lack of physical evidence.

- For Road, $S_{E,final}$ is equal to $S_{E,P}$ for the Sep-10 and Dec-11 EQs, whereas $S_{E,final}$ for the Feb-11 and Jun-11 EQs is a weighted average of $S_{E,L}$ and $S_{E,P}$ with respective weight coefficients of 1/3 and 2/3.
- The uncertainty associated with $S_{E,final}$ is also a weighted average of uncertainties associated with $S_{E,L}$ and $S_{E,P}$ with the same corresponding weights.
- The weights are based on the LiDAR error bands, LPI prediction error (Maurer et al. 2014[3]), presence of ejecta at the time of LiDAR surveys, and completeness of visual evidence (i.e., ground and aerial photographs and EQC LDAT property inspection reports for the site). The Warrington St site is in the apparent zone of higher ground surface subsidence for the Sep-10 EQ (i.e., the overestimate of ground surface elevation by July 2003 LiDAR survey). The site is in the zone of slight to moderate LPI overprediction of liquefaction severity for the Sep-10 EQ; it is in the zone of slight LPI underprediction to slight LPI overprediction of liquefaction severity for the Feb-11 EQ. The LDAT property inspection report is available for Patch A. There are no ground photographs of the road.

Summary 1:

- **The best estimate of the ejecta-induced free-field ground settlement at the Warrington St site for the SEP 2010, FEB 2011, and DEC 2011 earthquake is 0 mm, 40±10 mm, and 0 mm, respectively. There is insufficient visual evidence to determine the ejecta-induced free-field ground settlement for the JUN 2011 earthquake. However, it is estimated that the ejecta-induced settlement for the JUN 2011 earthquake is lower than that for the FEB 2011 earthquake. Considering the quantum of ejecta on the road and visible property lawns, the ejecta-induced settlement for the JUN 2011 can be estimated as 20±20 mm.**
- **The best estimate of the ejecta-induced settlement of the road at the Warrington St site for the SEP 2010, FEB 2011, JUN 2011, and DEC 2011 earthquake is 5±5 mm, 25±25 mm, 15±20 mm (mean = 15 mm, range = 0-35 mm), and <5 mm, respectively.**

Note 6: CPT 44959 was initially named as CC LIQ10.

[3] Maurer, B. W., Green, R. A., Cubrinovski, M., & Bradley, B. A. (2014). Evaluation of the Liquefaction Potential Index for Assessing Liquefaction Hazard in Christchurch, New Zealand. *Journal of Geotechnical and Geoenvironmental Engineering*, 140(7), 04014032-1-11. doi:10.1061/(asce)gt.1943-5606.0001117

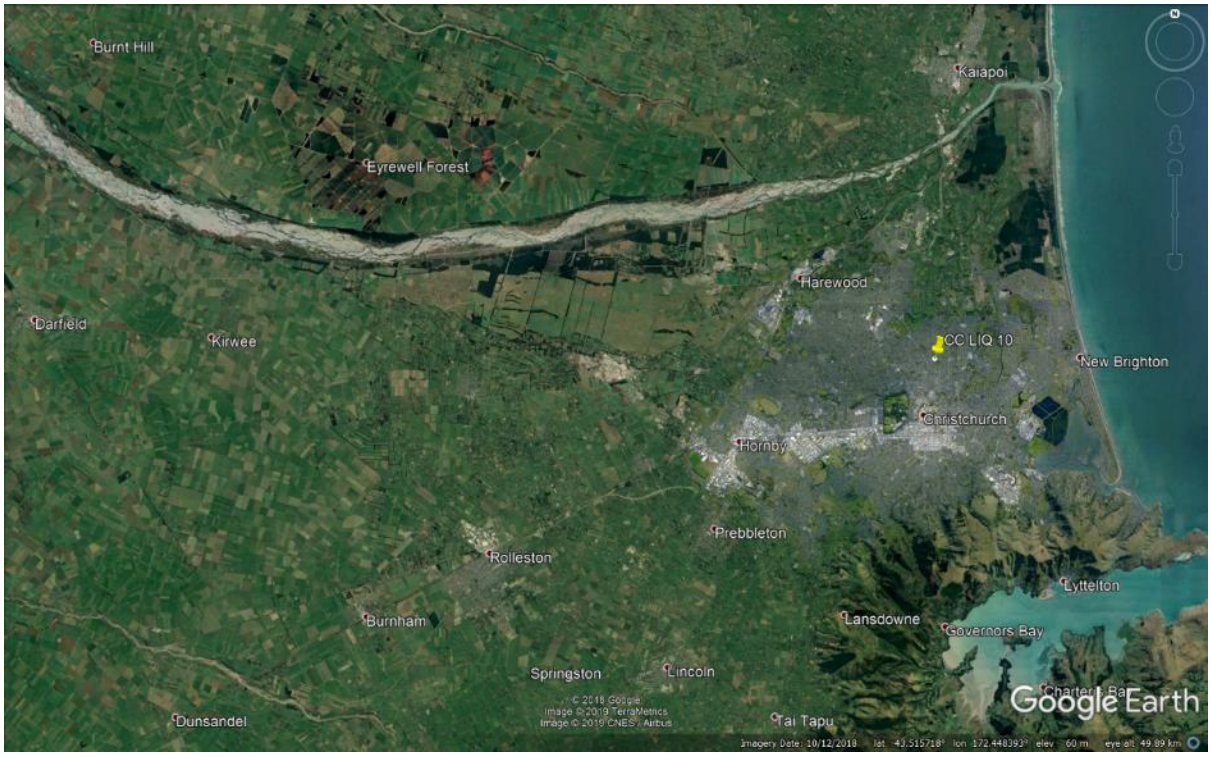

Figure 5: Location of the site.

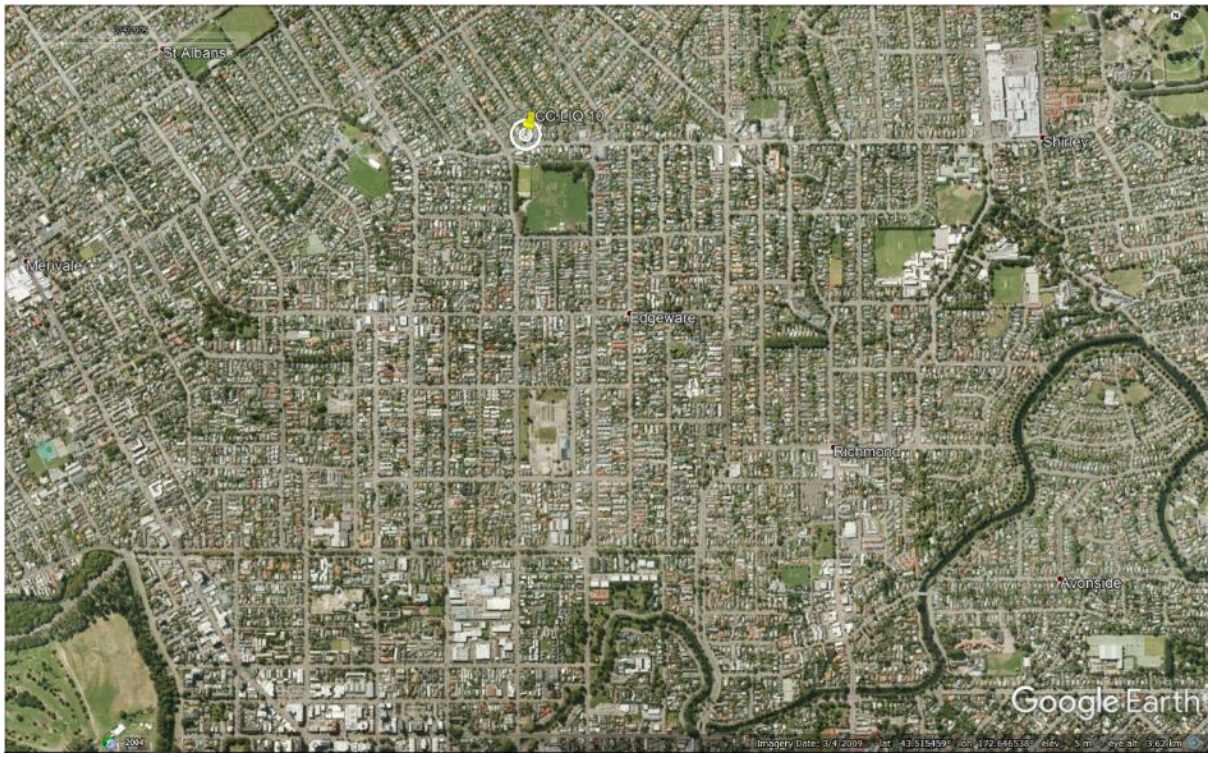

Figure 6: Position of the site relative to nearby buildings, vegetation, and free-face features.

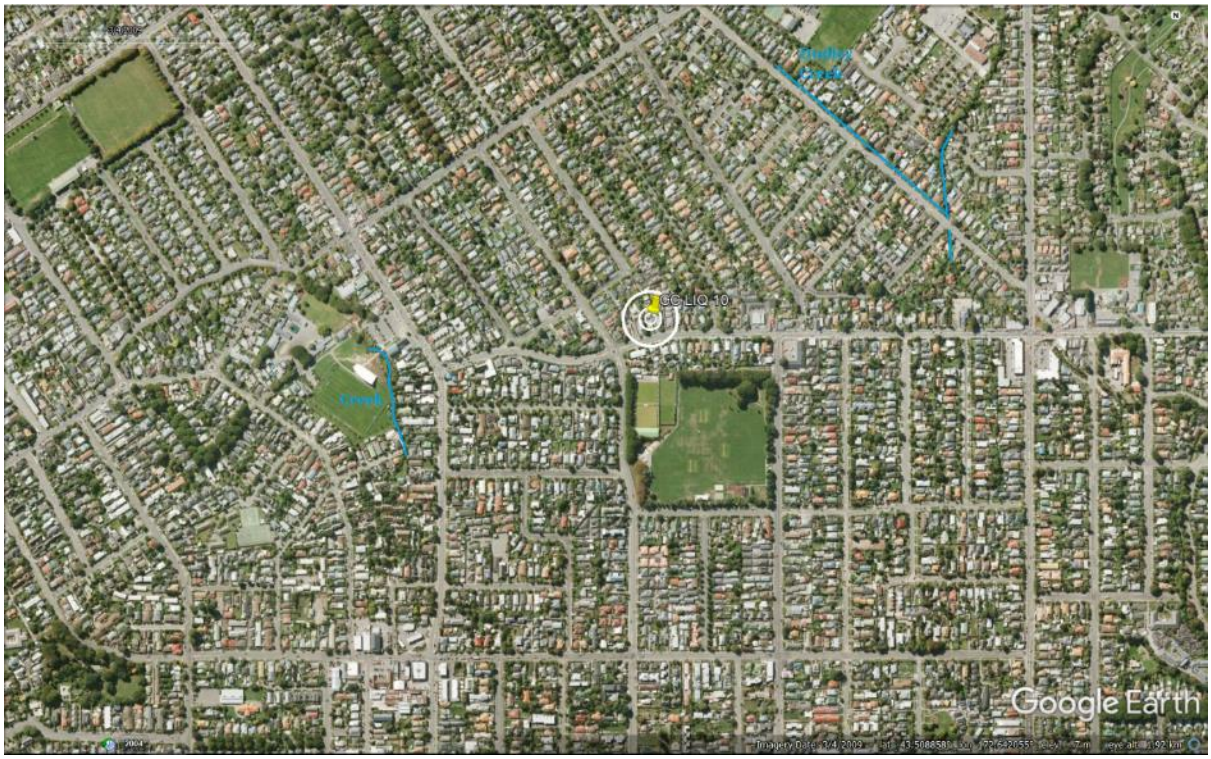

Figure 7: Position of the site relative to nearby free-face features.

Figure 8: Street view of the site showing flat land.

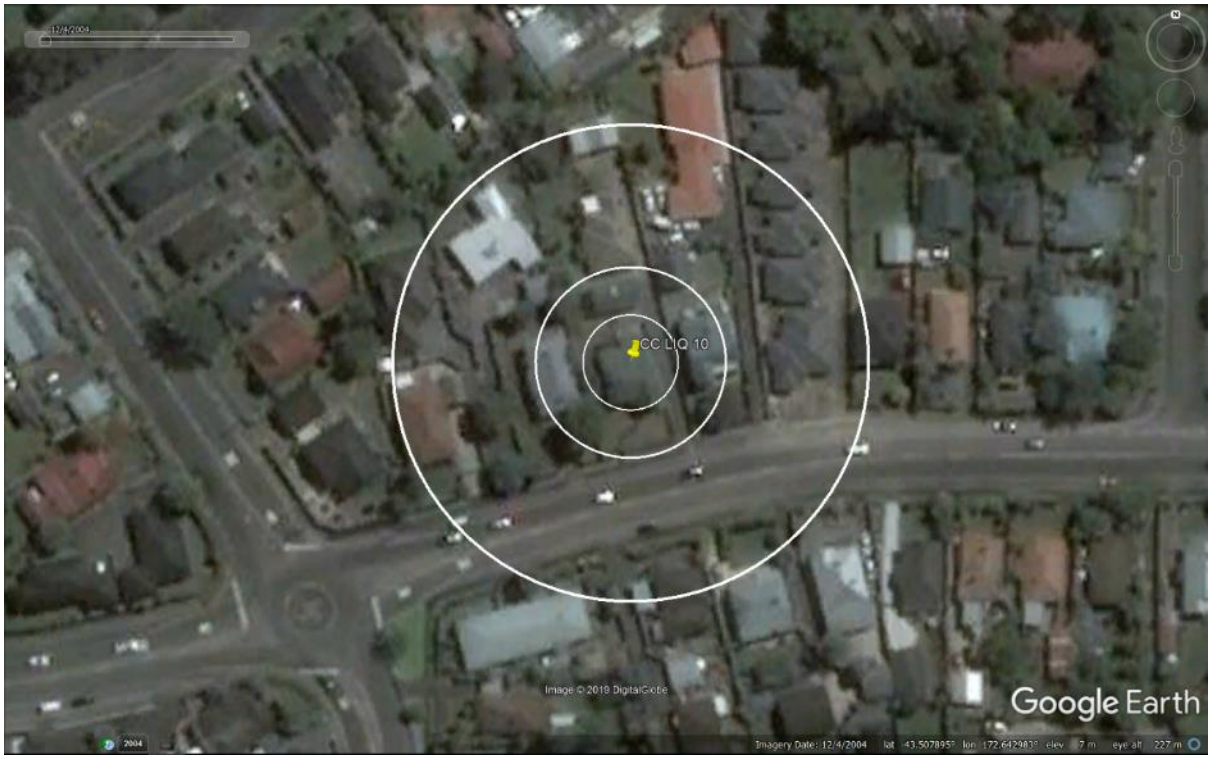

Figure 9: Satellite image of the site taken in Dec 2004.

Figure 10: Satellite image of the site taken in Mar 2009.

Figure 11: Satellite image of the site taken in Apr 2012.

Figure 12: Satellite image of the site taken in Jan 2016.

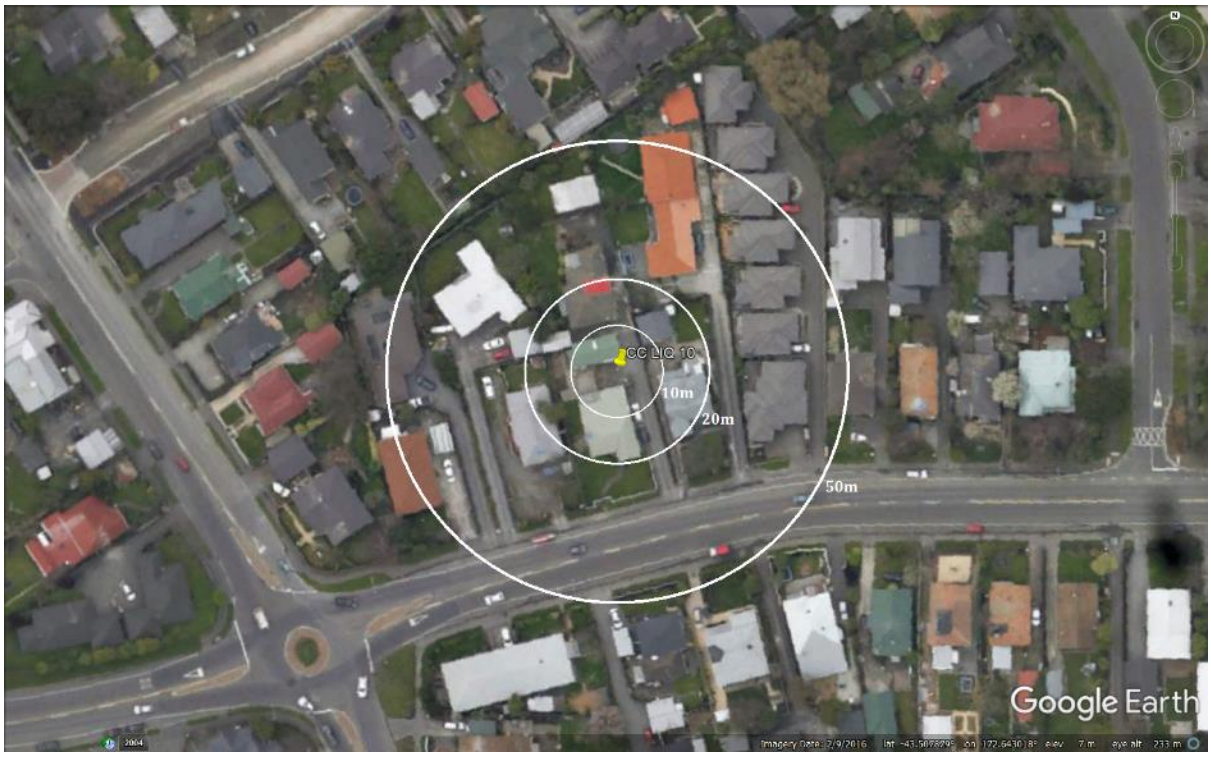

Figure 13: Aerial photograph of the site taken on Sep 4, 2010.

Figure 14: Aerial photograph of the site taken on Feb 24, 2011.

Figure 15: Aerial photograph of the site taken on June 14-15, 2011.

Figure 16: Aerial photograph of the site taken on June 16, 2011.

Figure 17: Aerial photograph of the site taken on Dec 24, 2011.

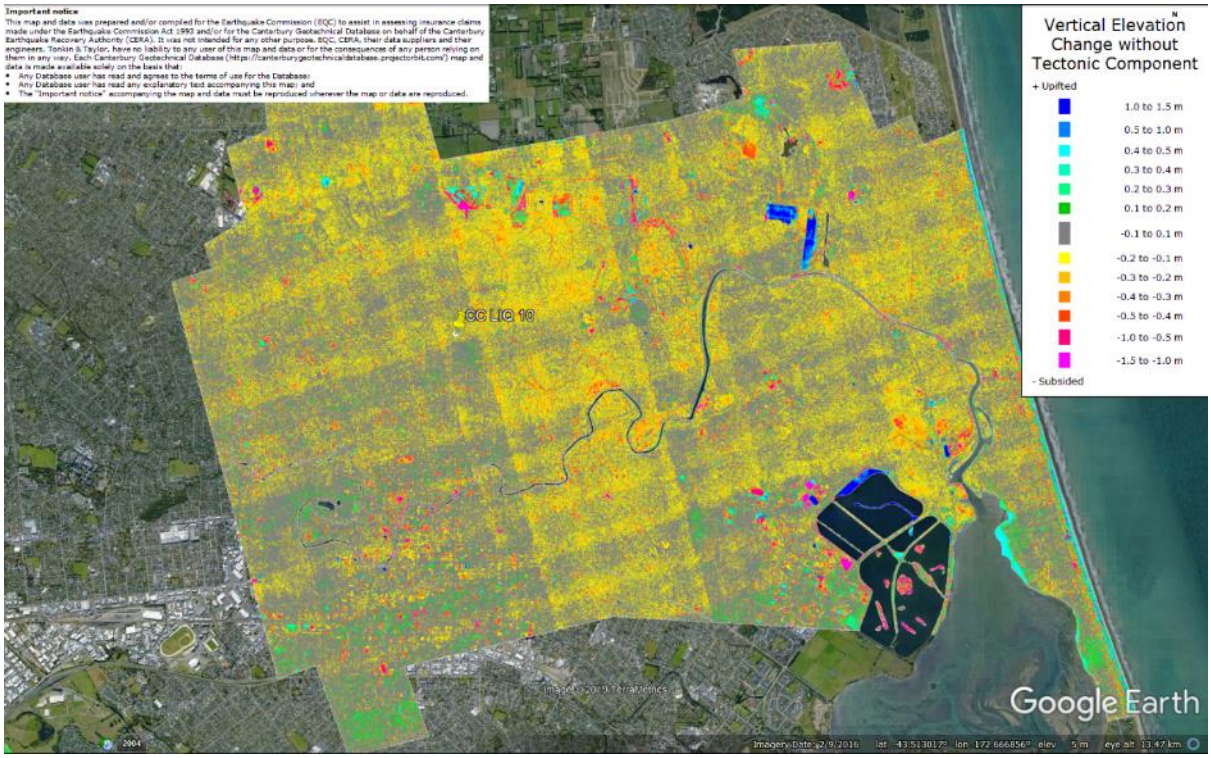

Figure 18: Vertical Ground Movements (Surface – Tectonic) for Sep 2010 Earthquake – the site is in the apparent zone of overestimated ground surface subsidence (e.g., July 2003 LIDAR flight error band).

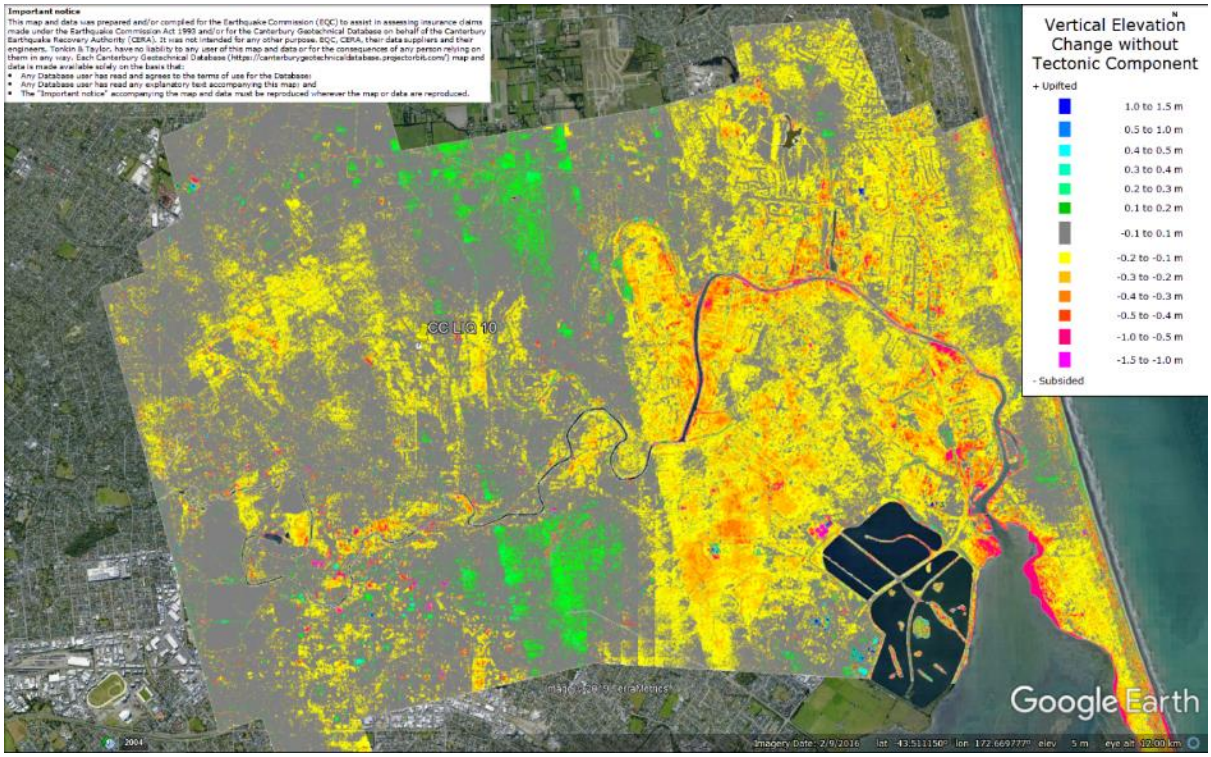

Figure 19: Vertical Ground Movements (Surface – Tectonic) for Feb 2011 Earthquake – the site is not in the apparent zone of underestimated ground surface subsidence.

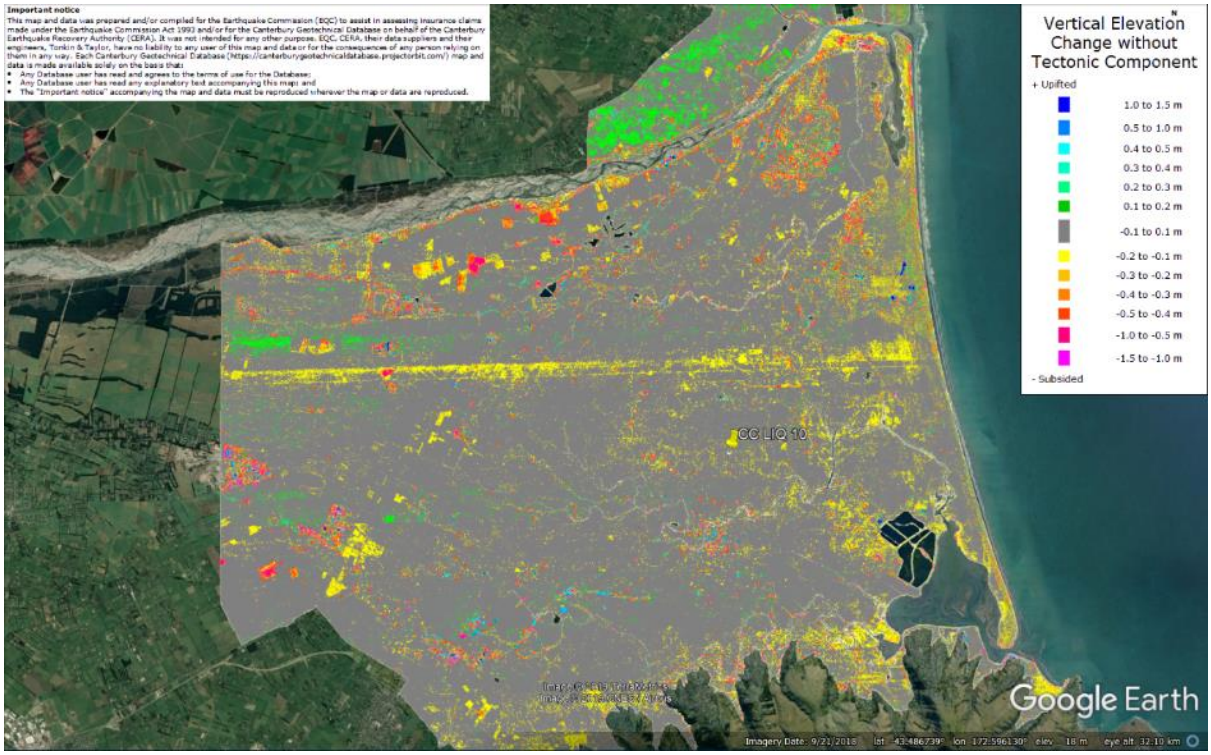

Figure 20: Vertical Ground Movements (Surface – Tectonic) for June 2011 Earthquake – the site is not in the apparent zone of overestimated or underestimated ground surface subsidence.

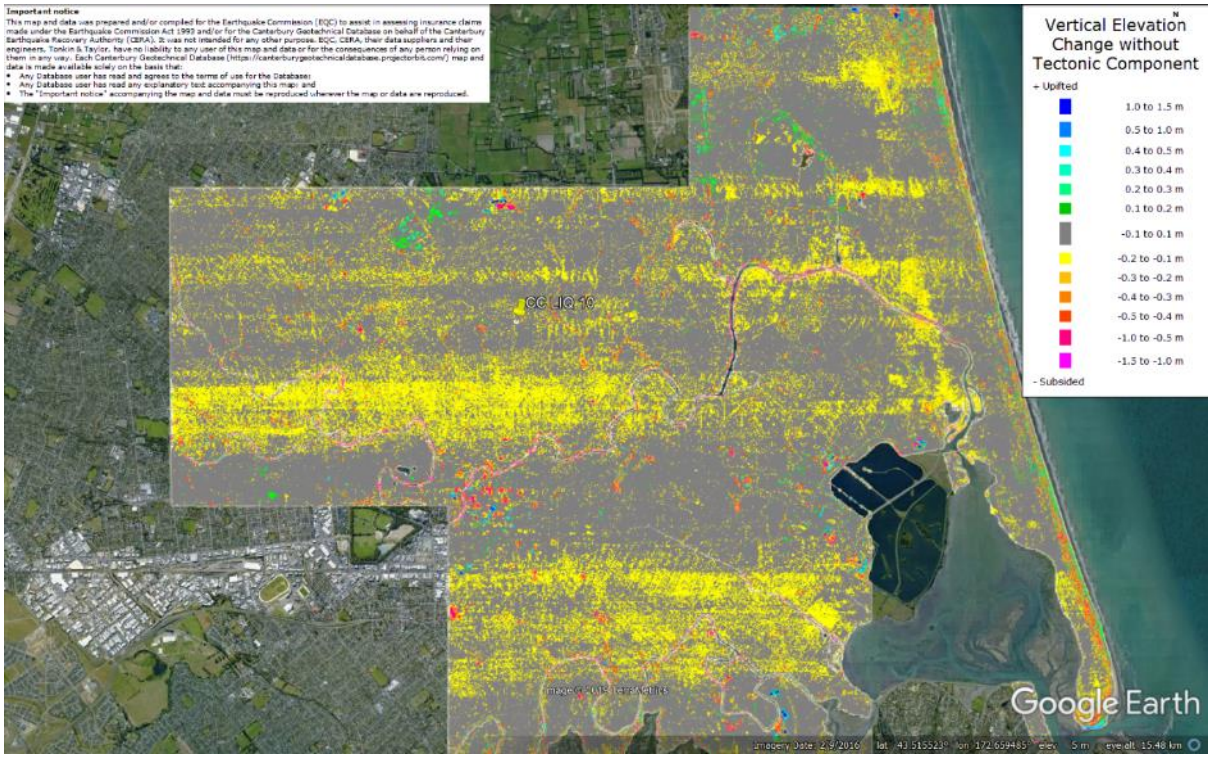

Figure 21: Vertical Ground Movements (Surface – Tectonic) for Dec 2011 Earthquake – the site is not in the apparent zone of overestimated or underestimated ground surface subsidence.

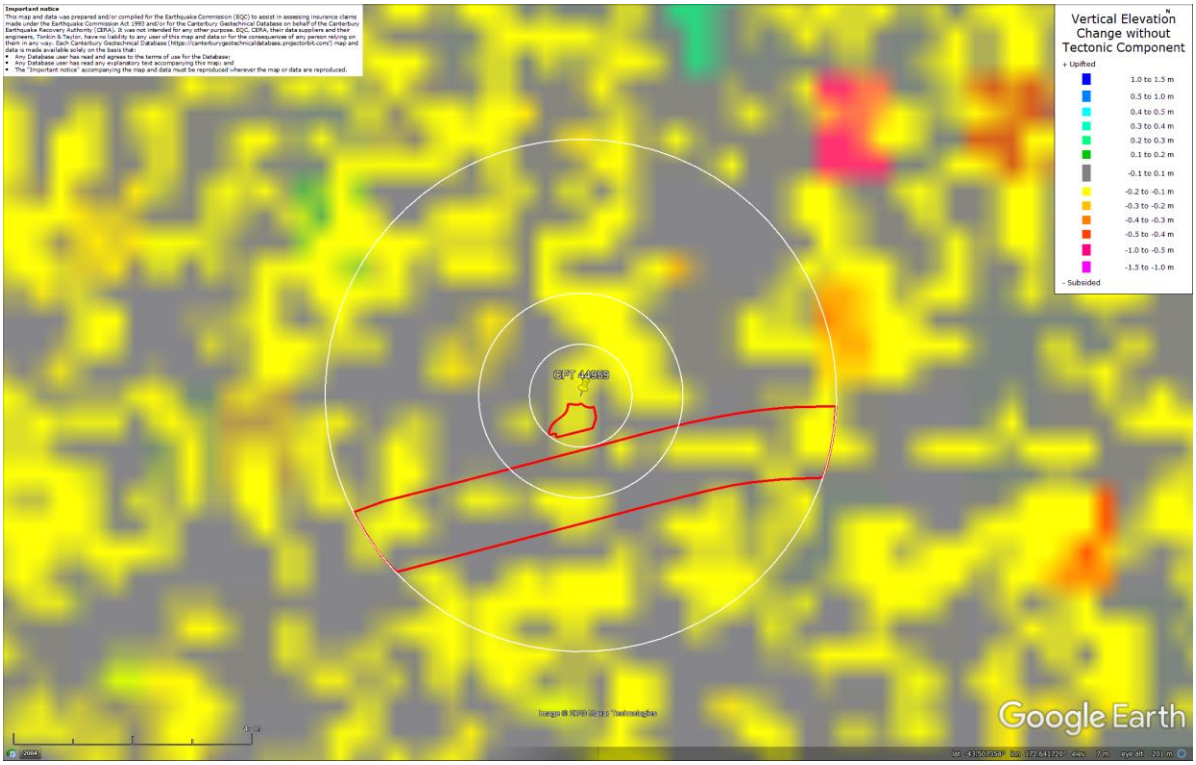

Figure 22: Ground surface subsidence without tectonic component for Sep 2010 Earthquake according to the LiDAR DEM.

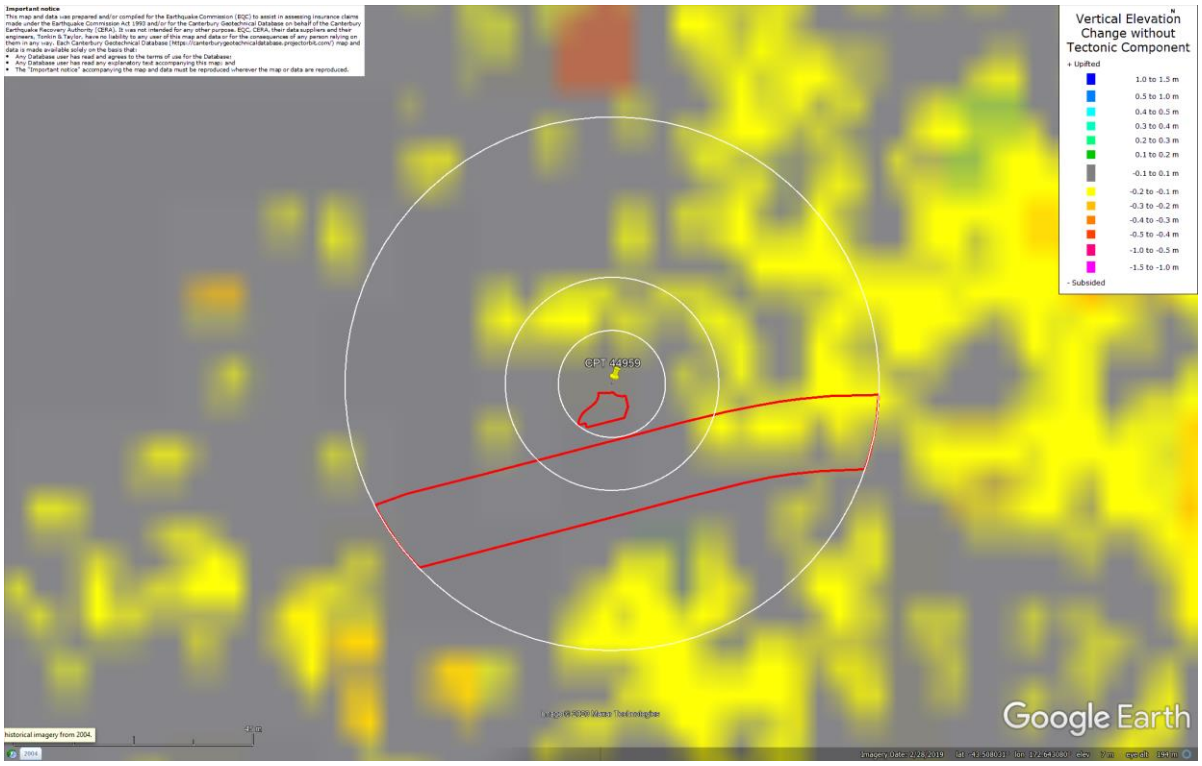

Figure 23: Ground surface subsidence without tectonic component for Feb 2011 Earthquake according to the LiDAR DEM.

Figure 24: Ground surface subsidence without tectonic component for Jun 2011 Earthquake according to the LiDAR DEM.

Figure 25: Ground surface subsidence without tectonic component for Dec 2011 Earthquake according to the LiDAR DEM.

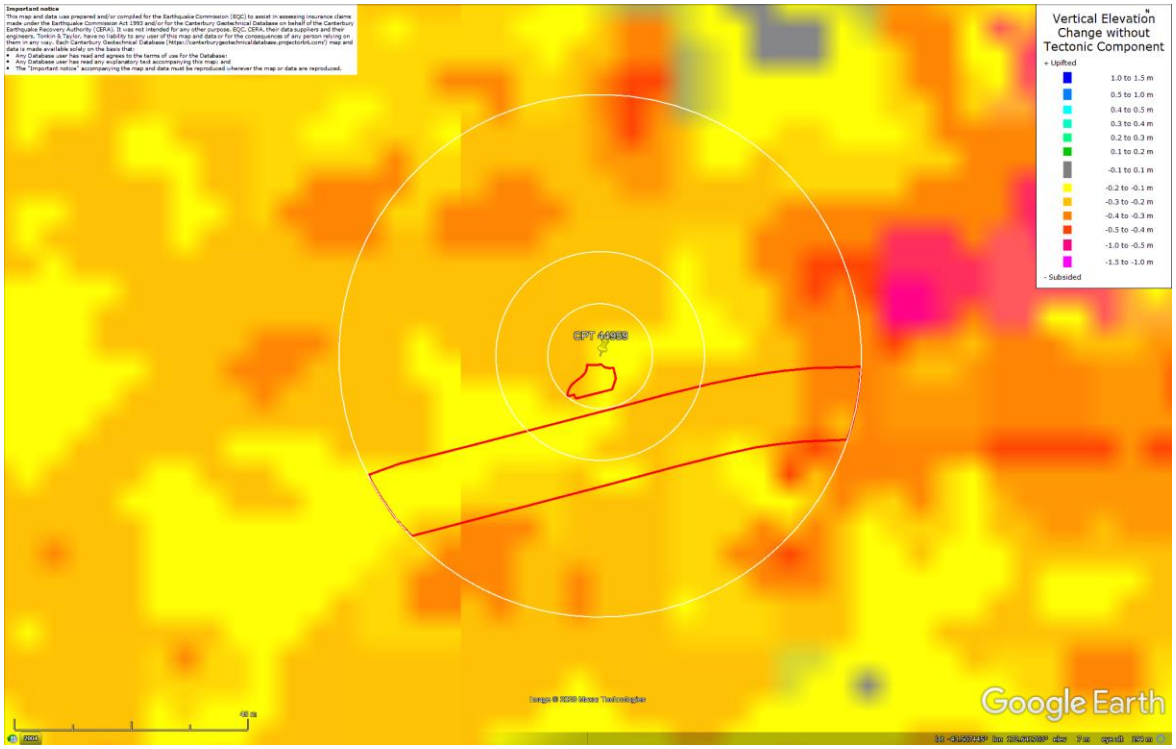

Figure 26: Ground surface subsidence without tectonic component for Canterbury Earthquake Sequence according to the LiDAR DEM.

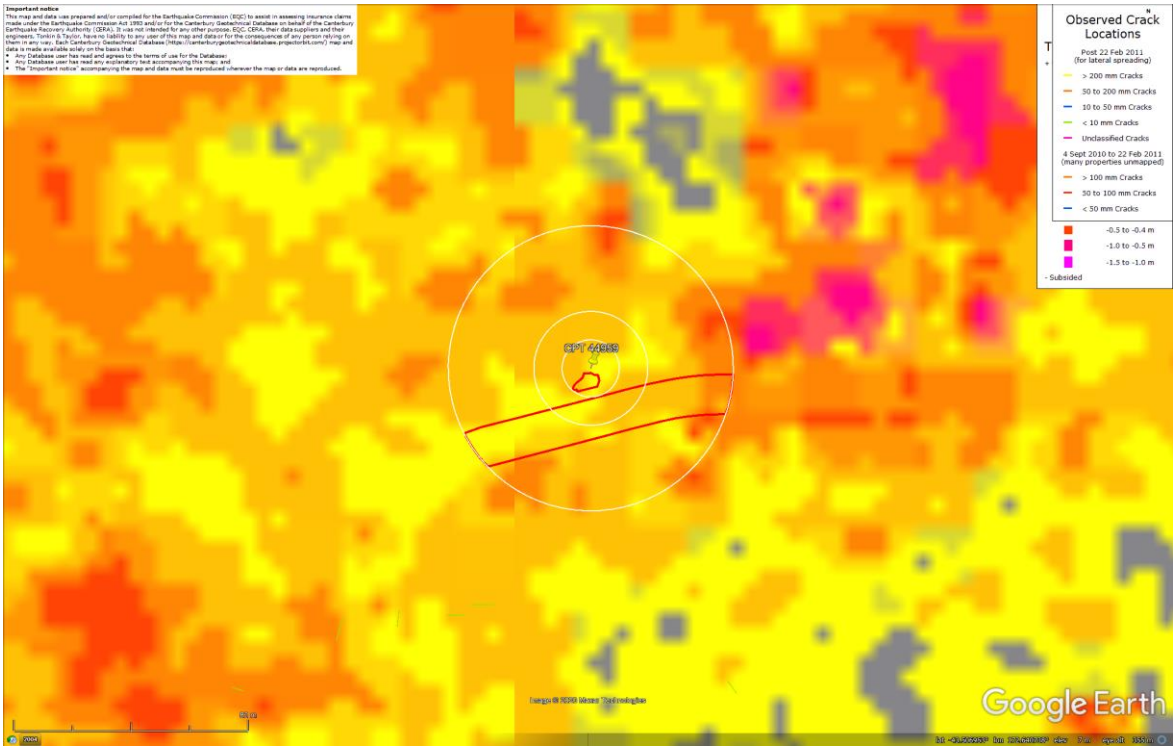

Figure 27: Absence of ground cracks indicates no lateral spreading for Canterbury Earthquake Sequence.

Figure 28: Vertical tectonic movements for Sep 2010 Earthquake.

Figure 29: Vertical tectonic movements for Feb 2011 Earthquake.

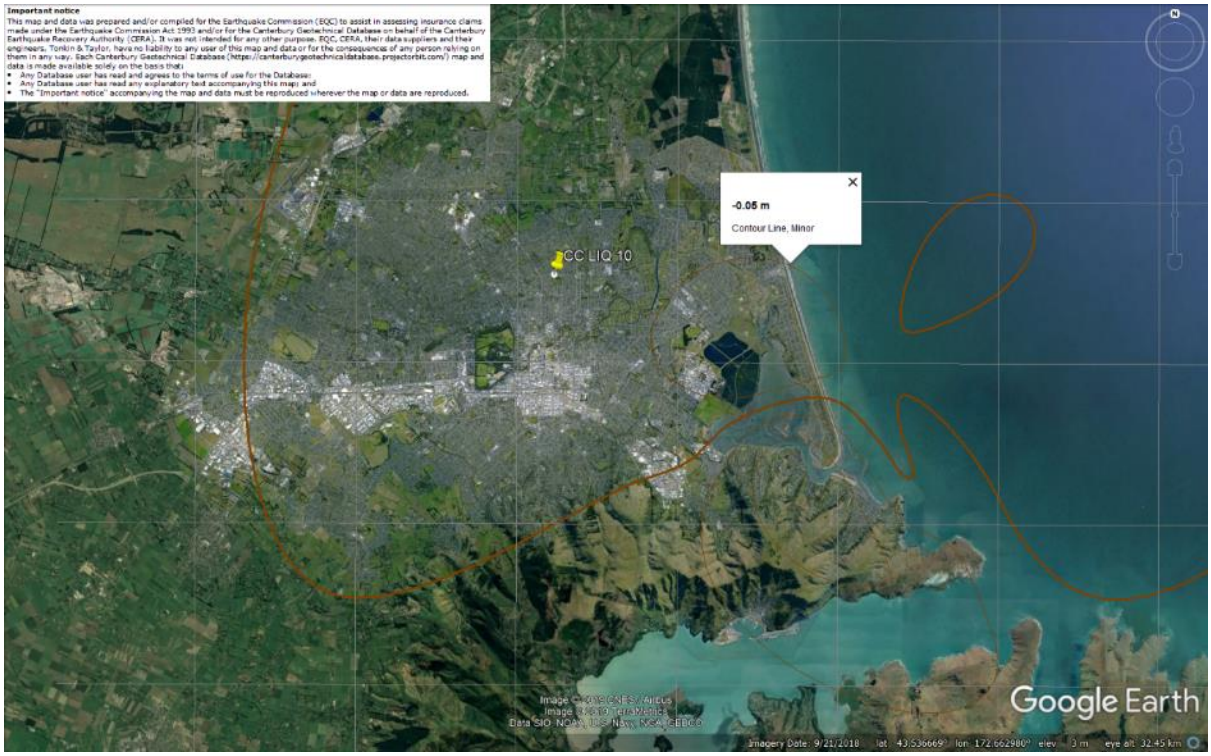

Figure 30: Vertical tectonic movements for June 2011 Earthquake.

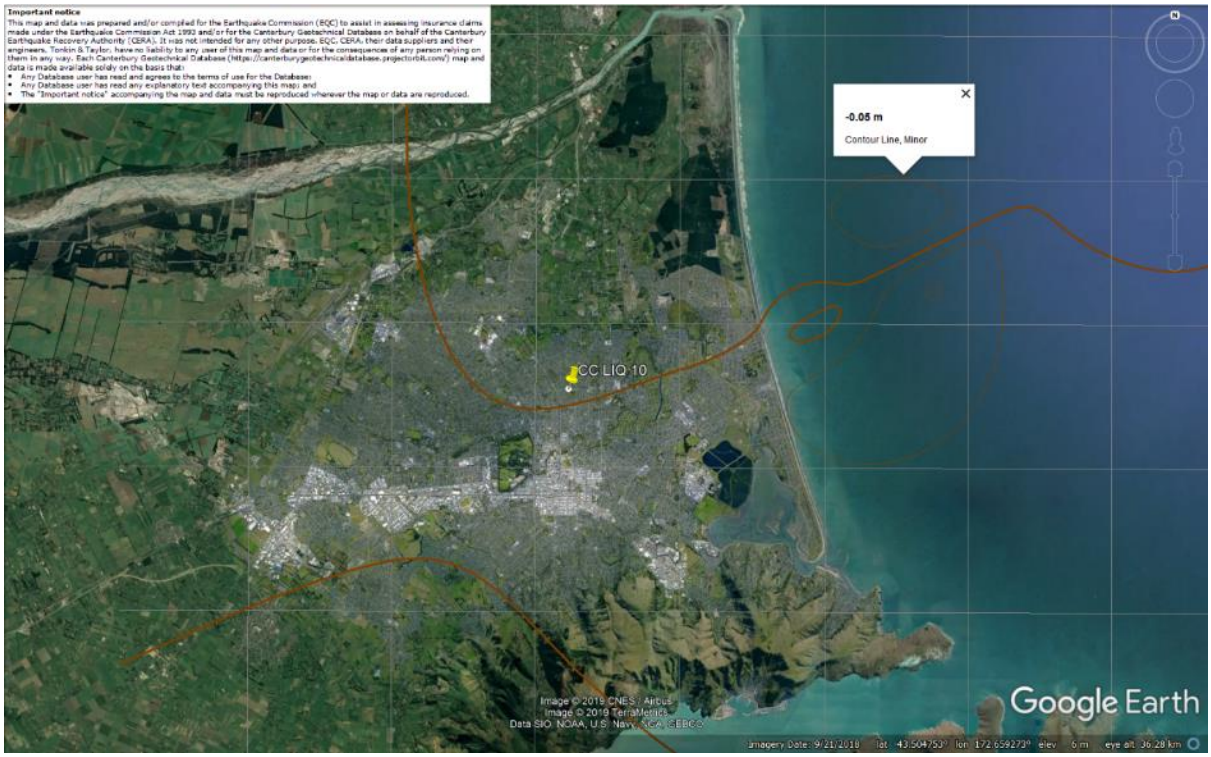

Figure 31: Vertical tectonic movements for Dec 2011 Earthquake.

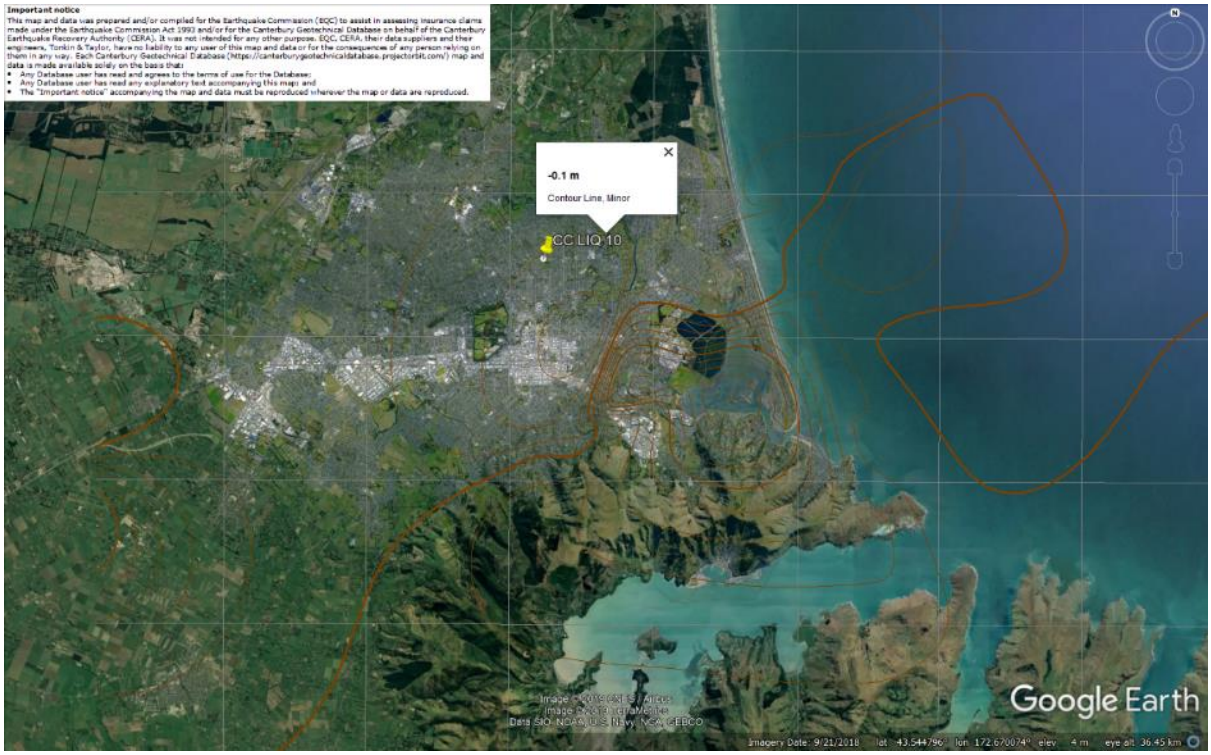

Figure 32: Vertical tectonic movements for Canterbury Earthquake Sequence.

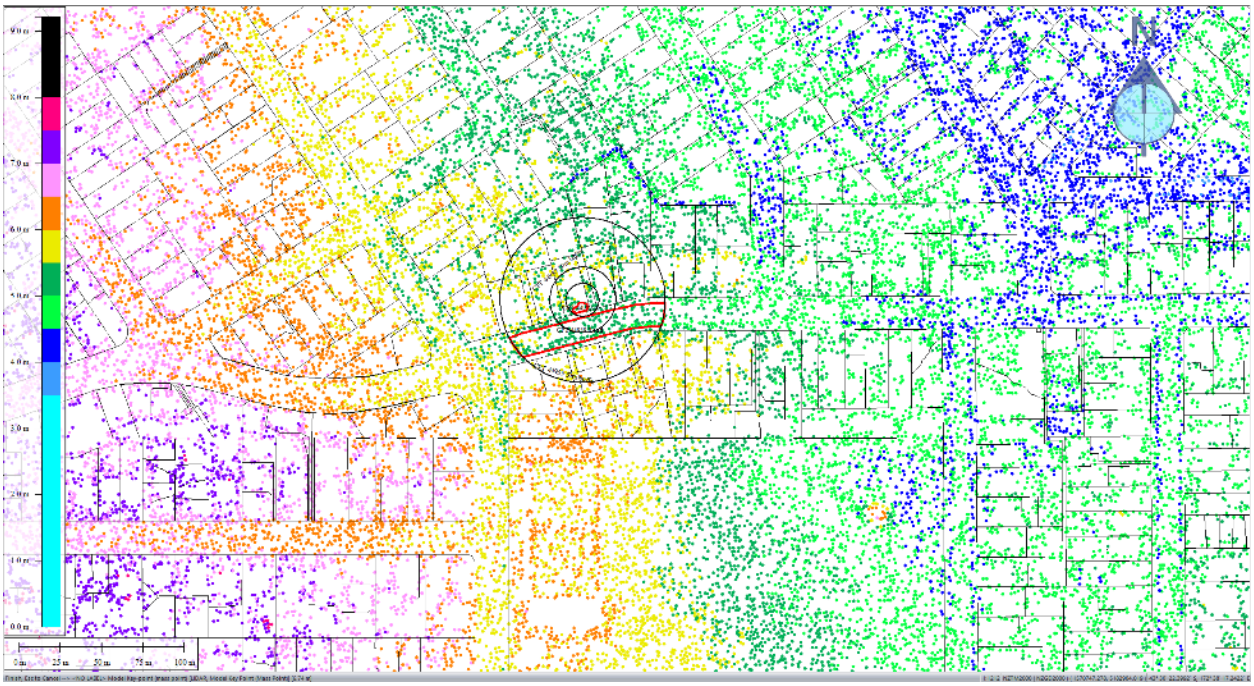

Figure 33: Jul 2003 LiDAR survey.

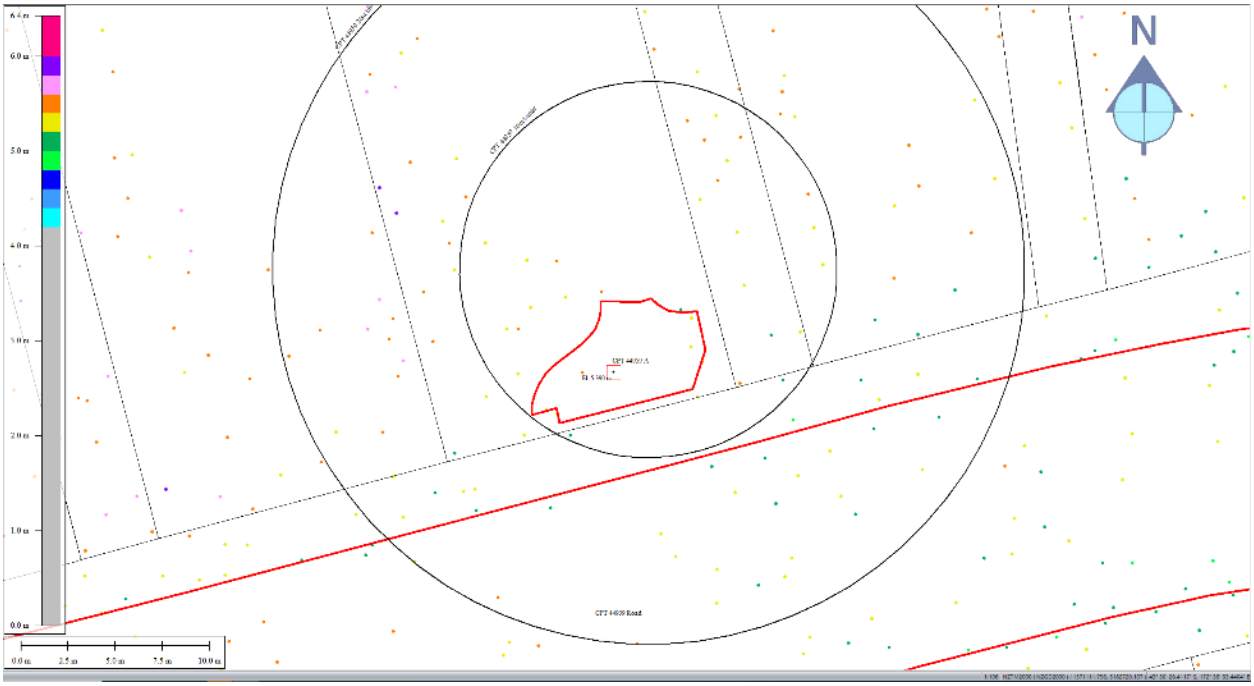

Figure 34: Ground surface elevation averaged over Patch A for Jul 2003 LiDAR survey.

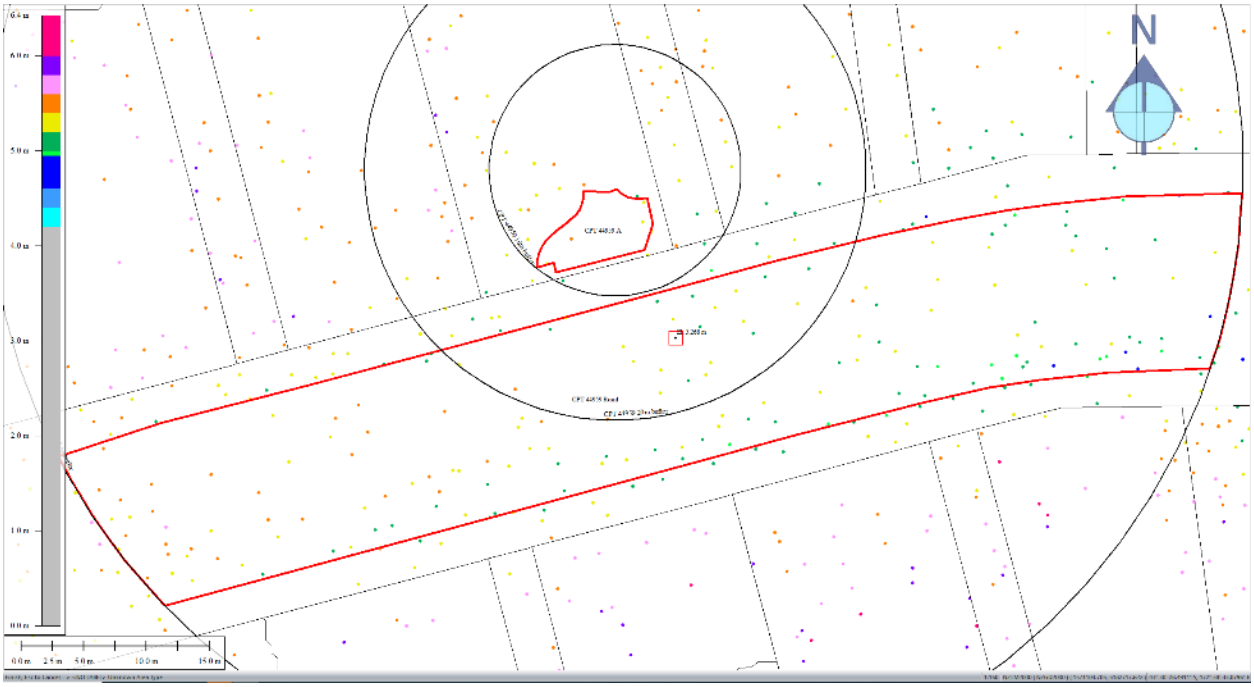

Figure 35: Ground surface elevation average over the 20-m buffer for Road for Jul 2003 LiDAR survey.

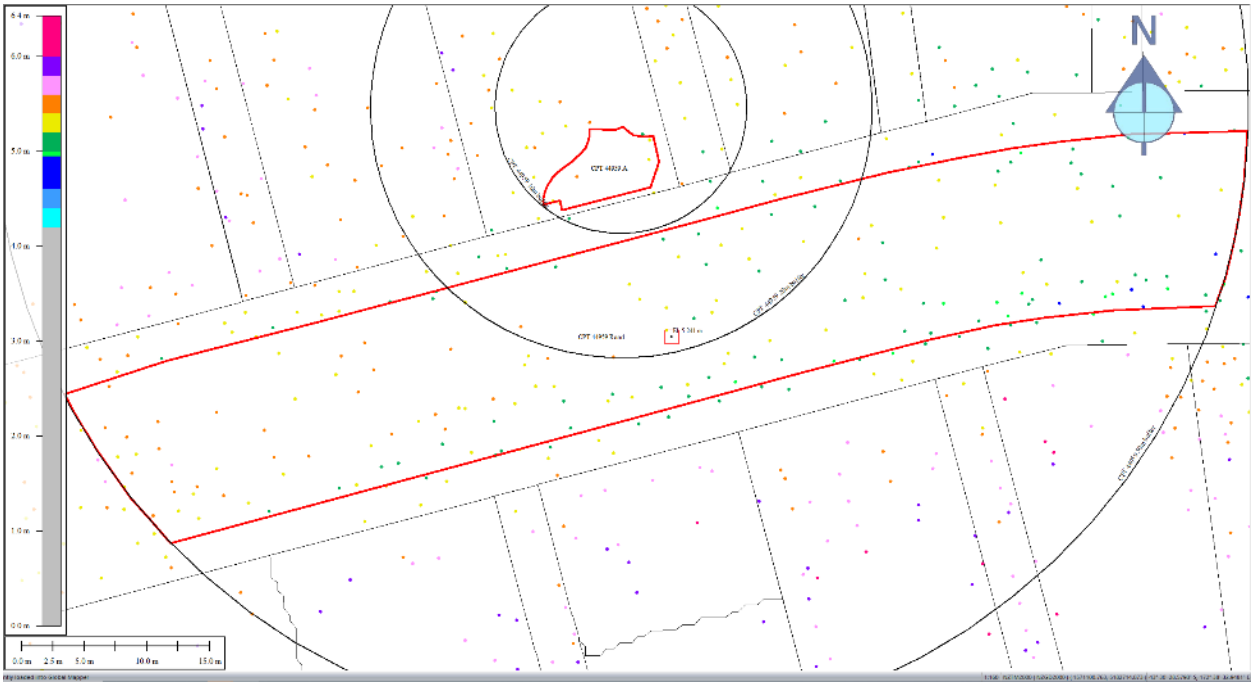

Figure 36: Ground surface elevation average over the 50-m buffer for Road for Jul 2003 LiDAR survey.

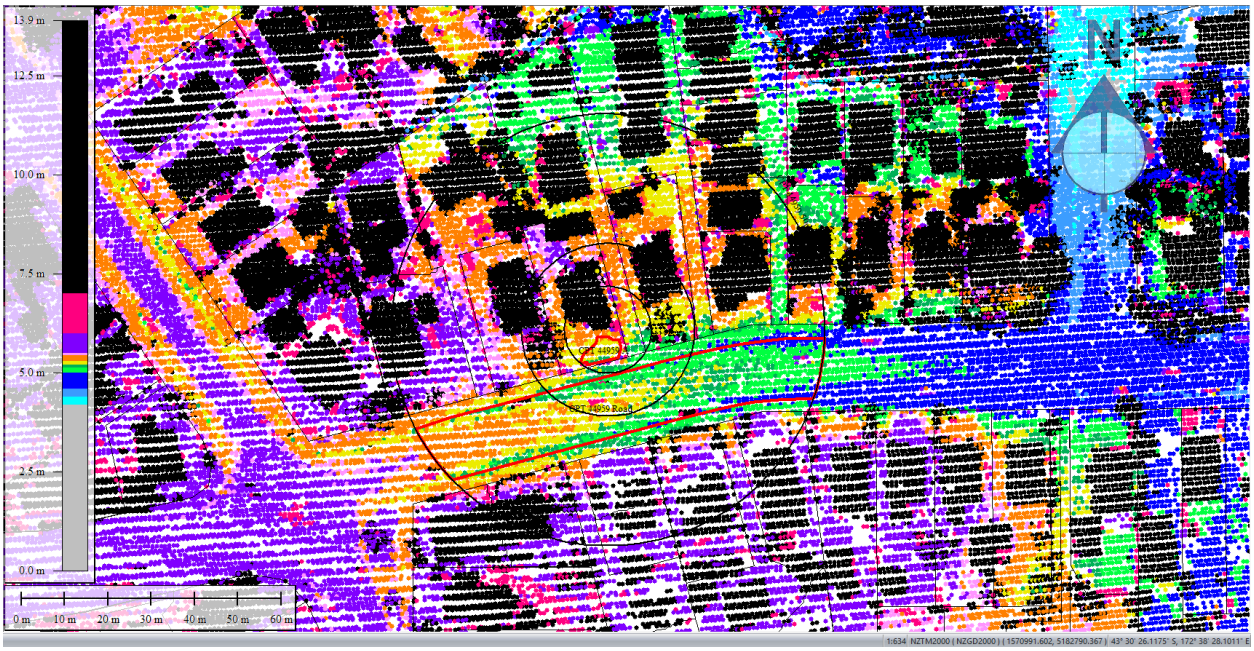

Figure 37: Sep 5, 2010 LiDAR survey.

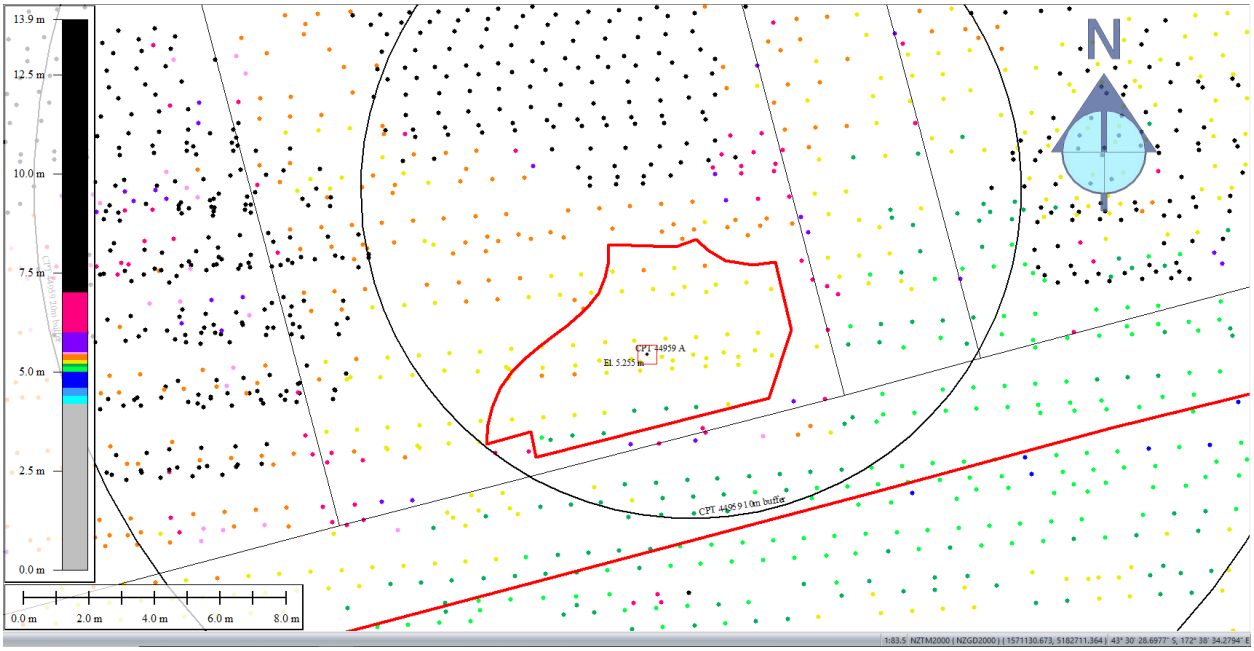

Figure 38: Ground surface elevation averaged over Patch A for Sep 5, 2010 LiDAR survey.

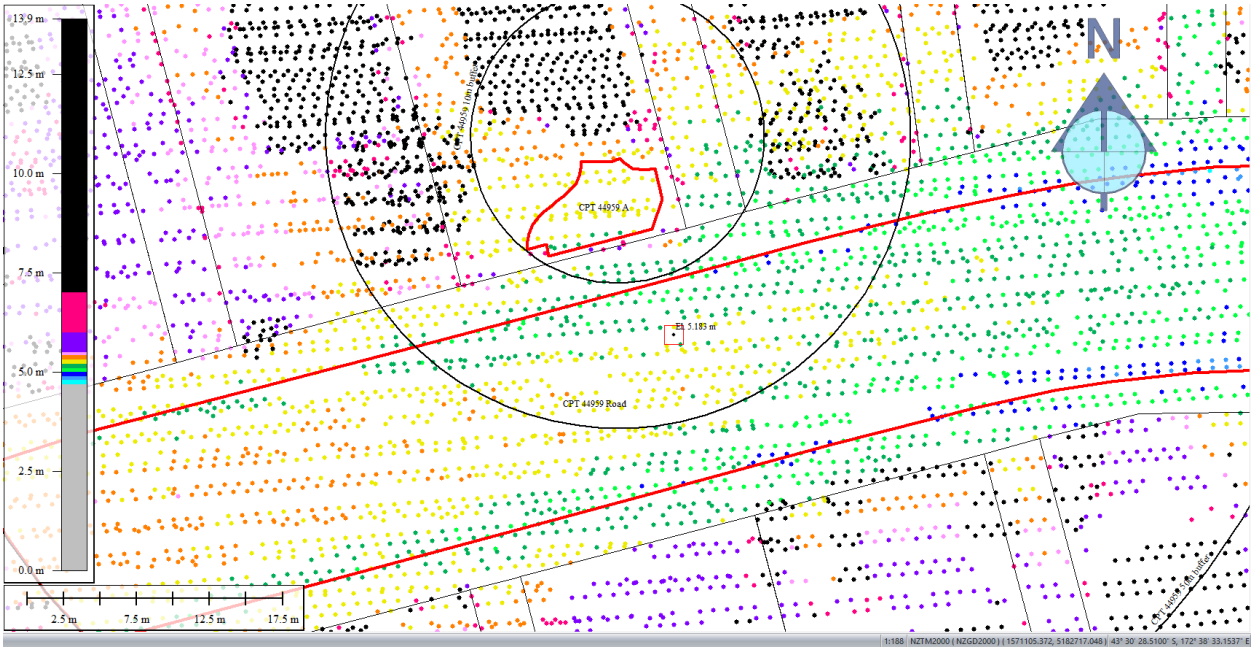

Figure 39: Ground surface elevation averaged over the 20-m buffer for Road for Sep 5, 2010 LiDAR survey.

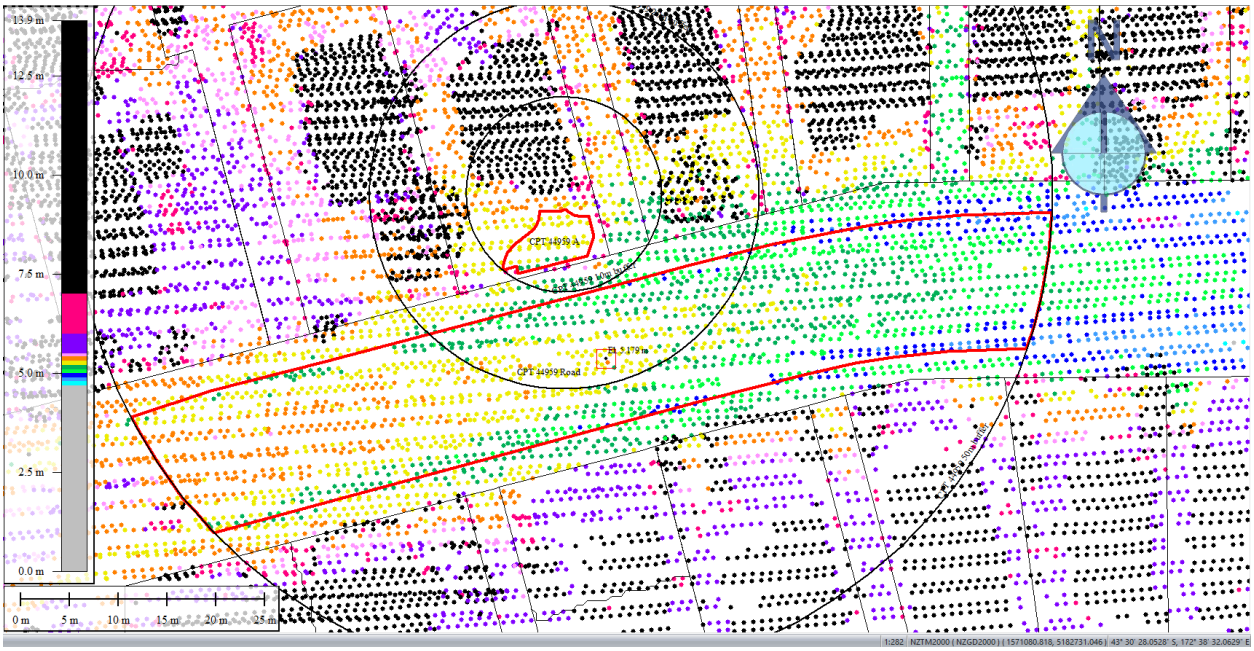

Figure 40: Ground surface elevation averaged over the 50-m buffer for Road for Sep 5, 2010 LiDAR survey.

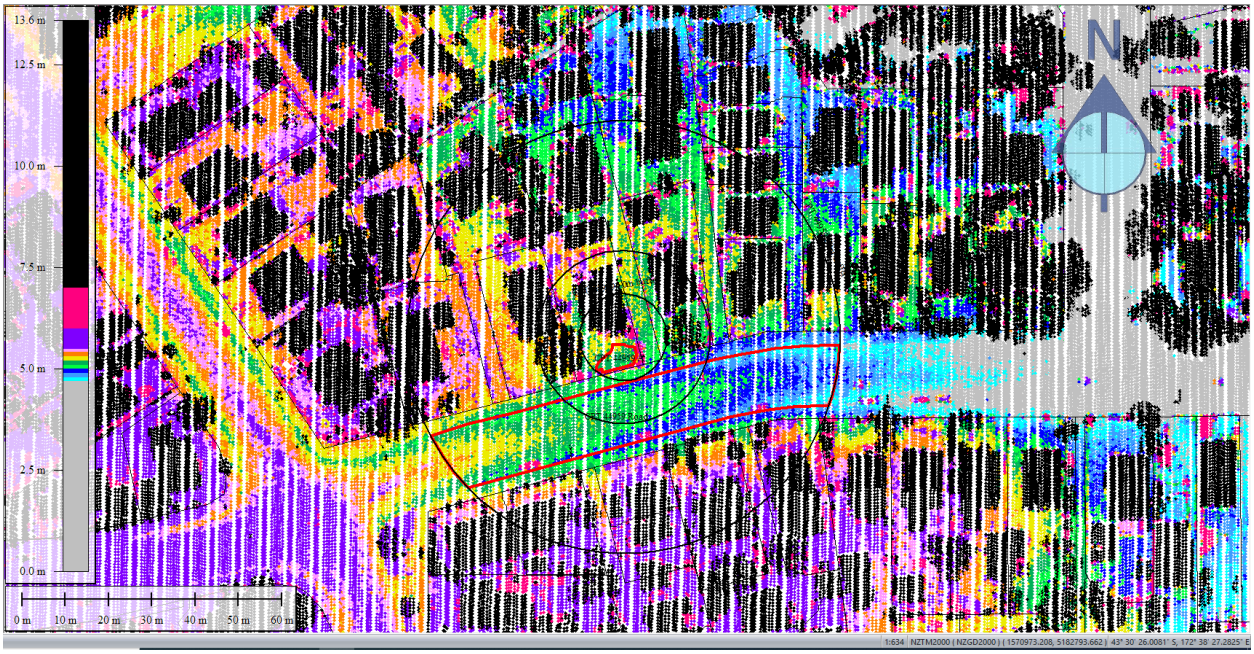

Figure 41: Mar 2011 LiDAR survey.

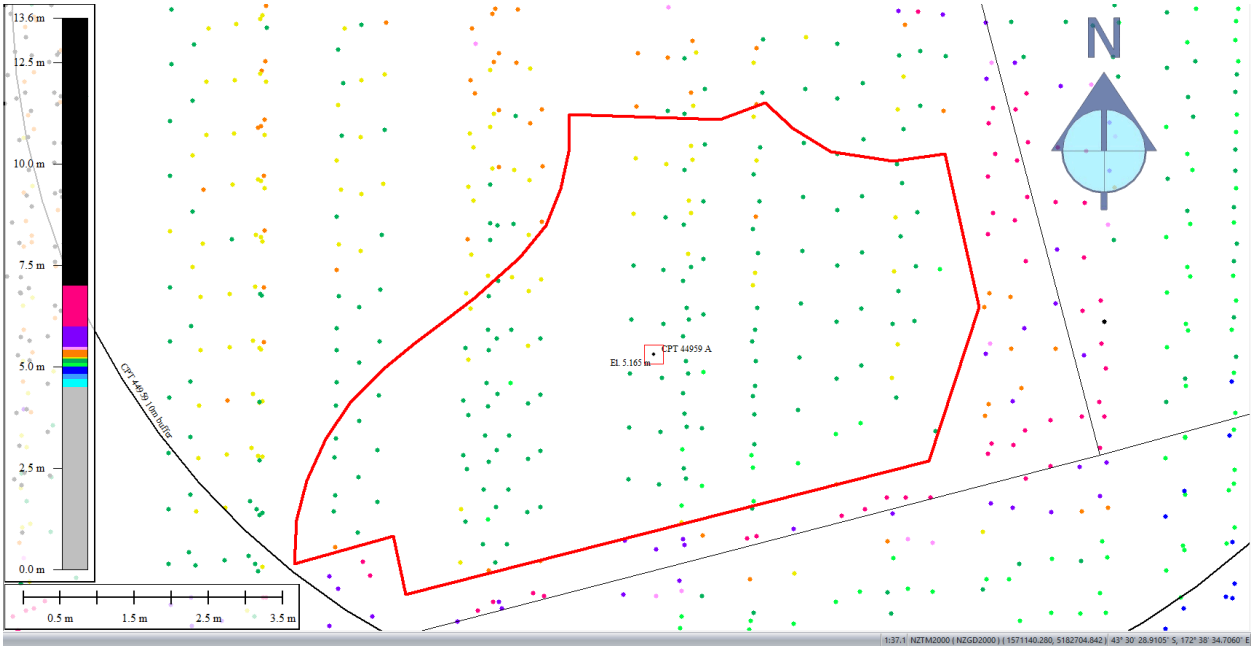

Figure 42: Ground surface elevation averaged over Patch A for Mar 2011 LiDAR survey.

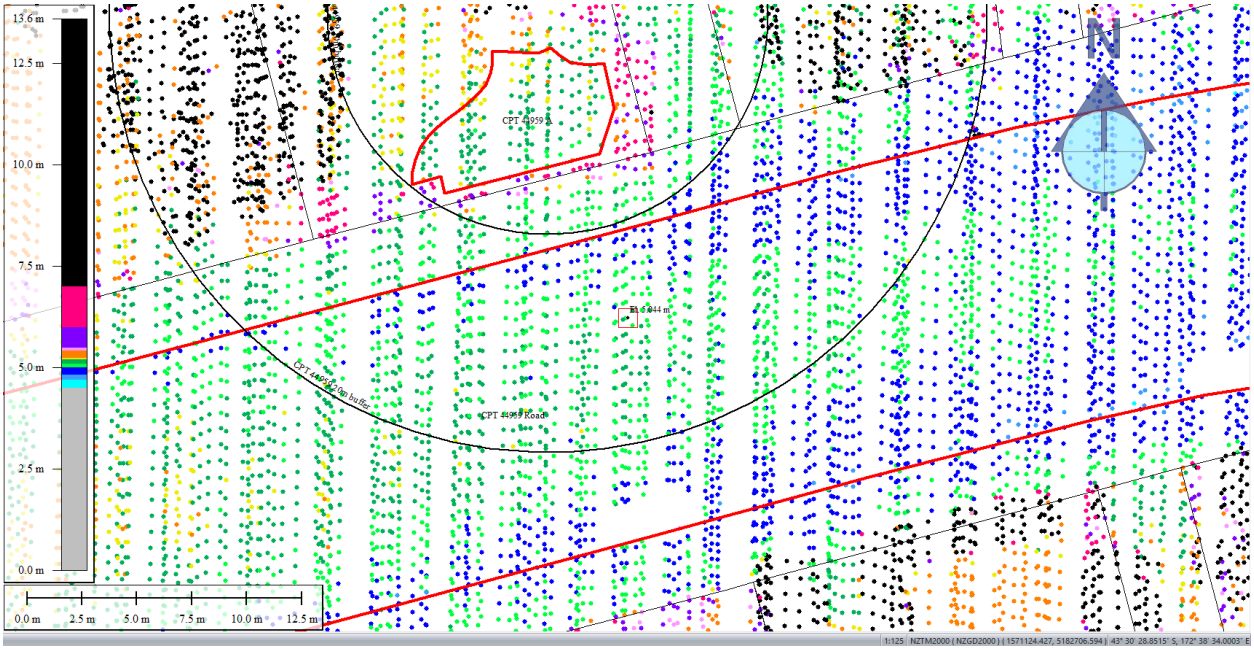

Figure 43: Ground surface elevation averaged over the 20-m buffer for Road for Mar 2011 LiDAR survey.

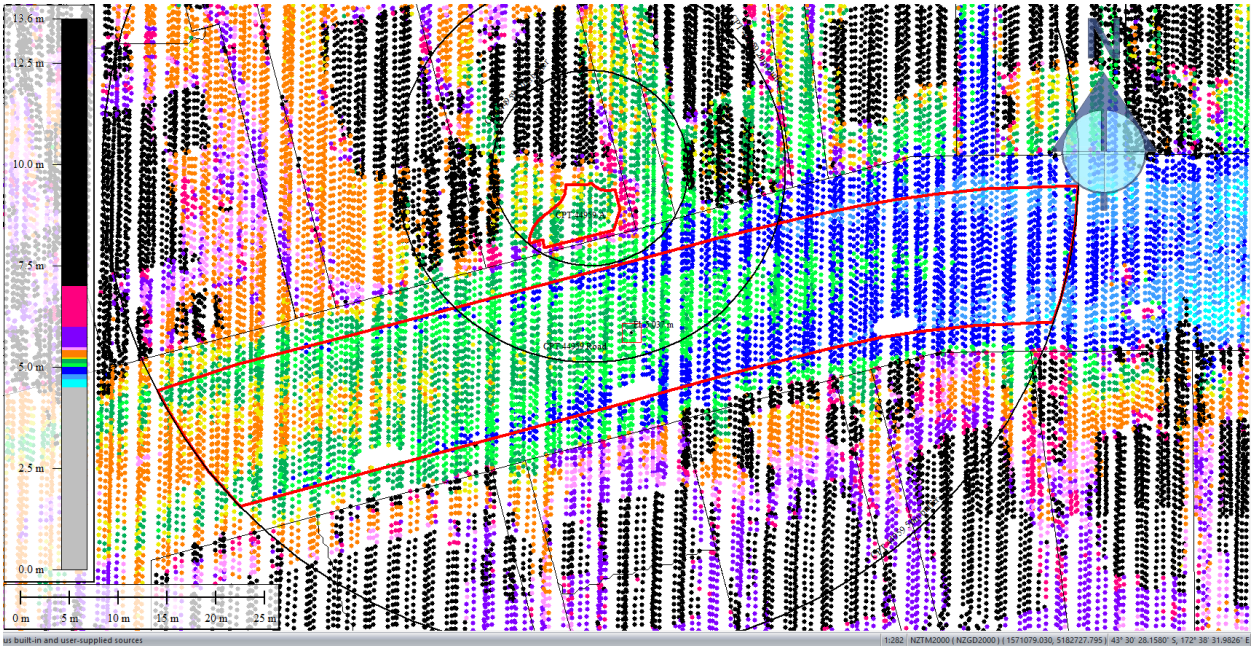

Figure 44: Ground surface elevation averaged over the 50-m buffer for Road for Mar 2011 LiDAR survey.

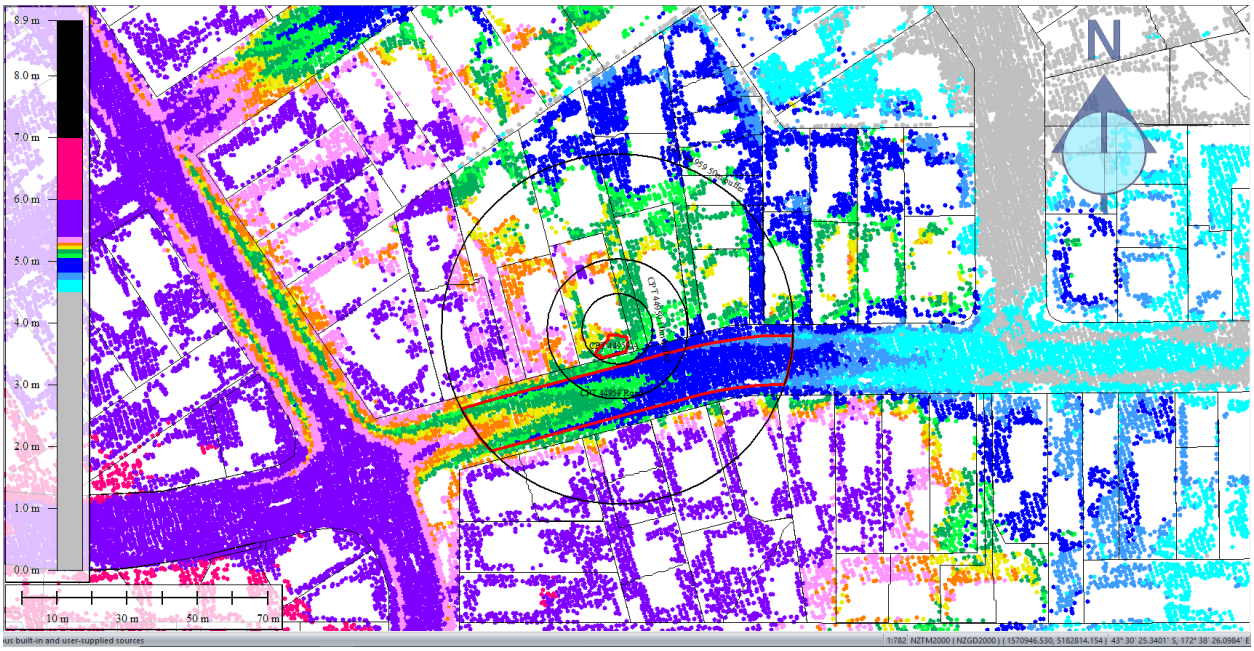

Figure 45: May 2011 LiDAR survey.

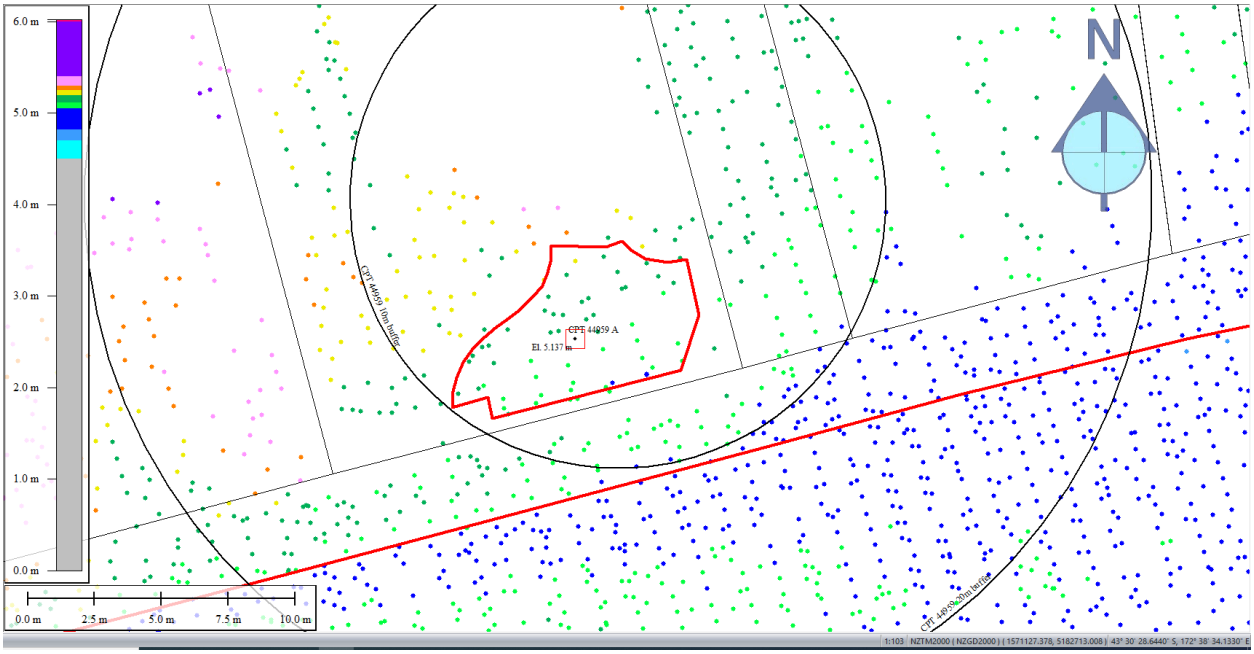

Figure 46: Ground surface elevation averaged over Patch A for May 2011 LiDAR survey.

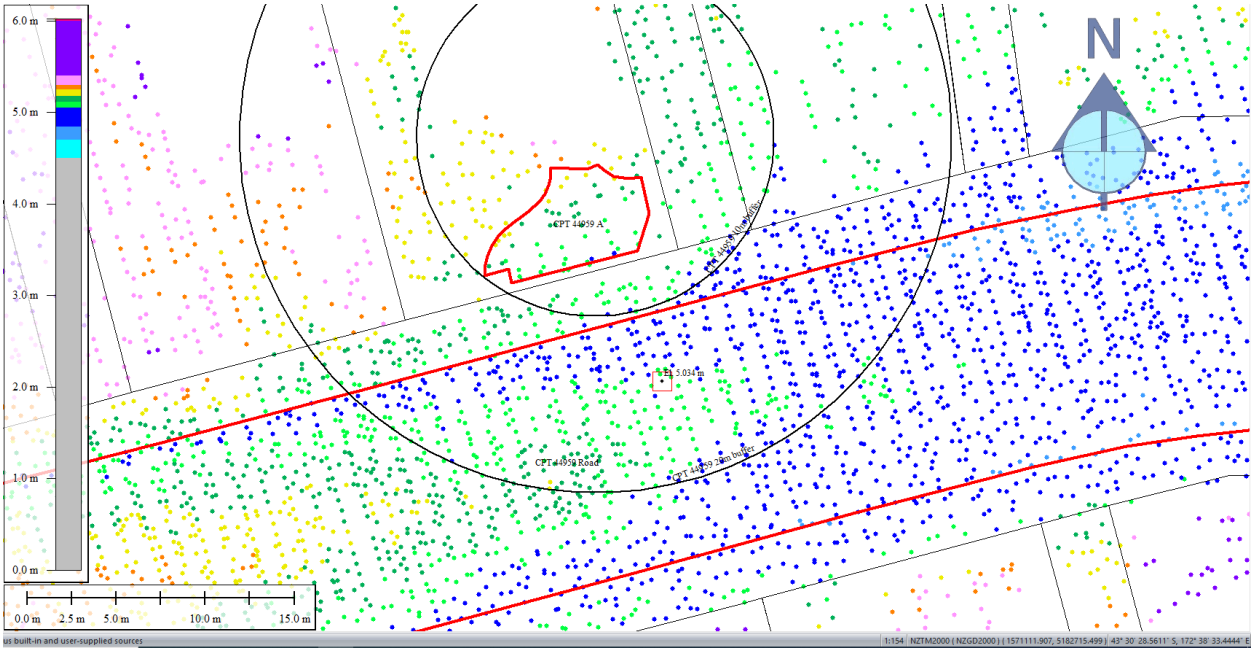

Figure 47: Ground surface elevation averaged over the 20-m buffer for Road for May 2011 LiDAR survey.

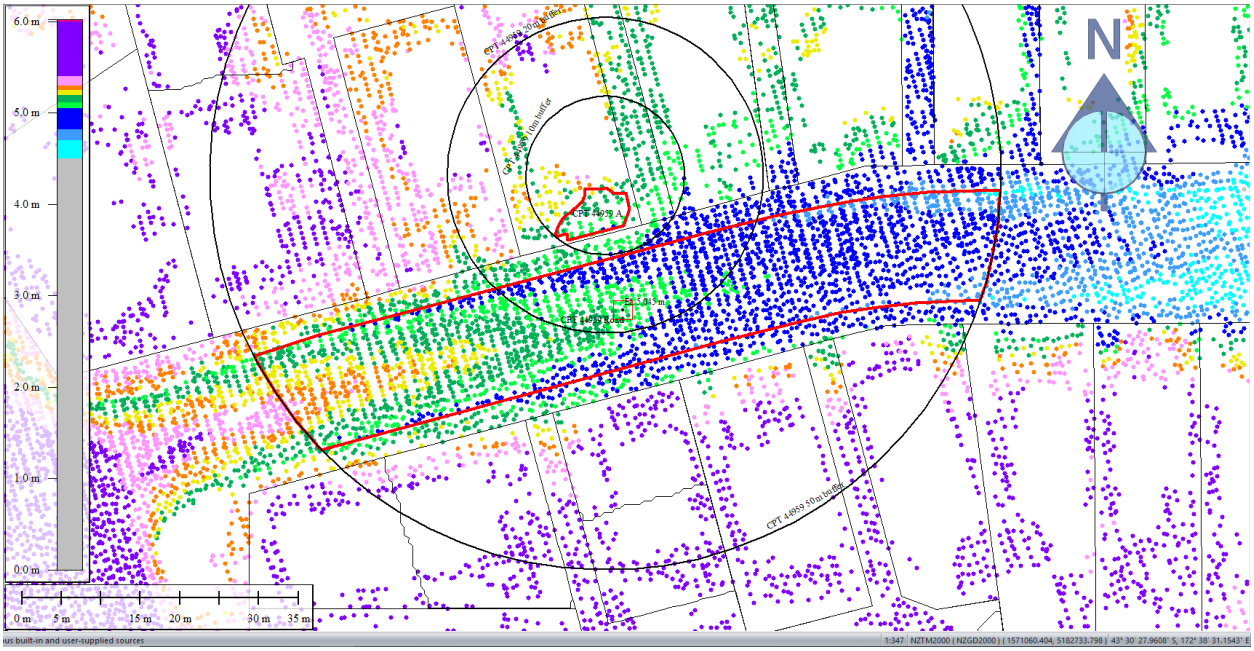

Figure 48: Ground surface elevation averaged over the 50-m buffer for Road for May 2011 LiDAR survey.

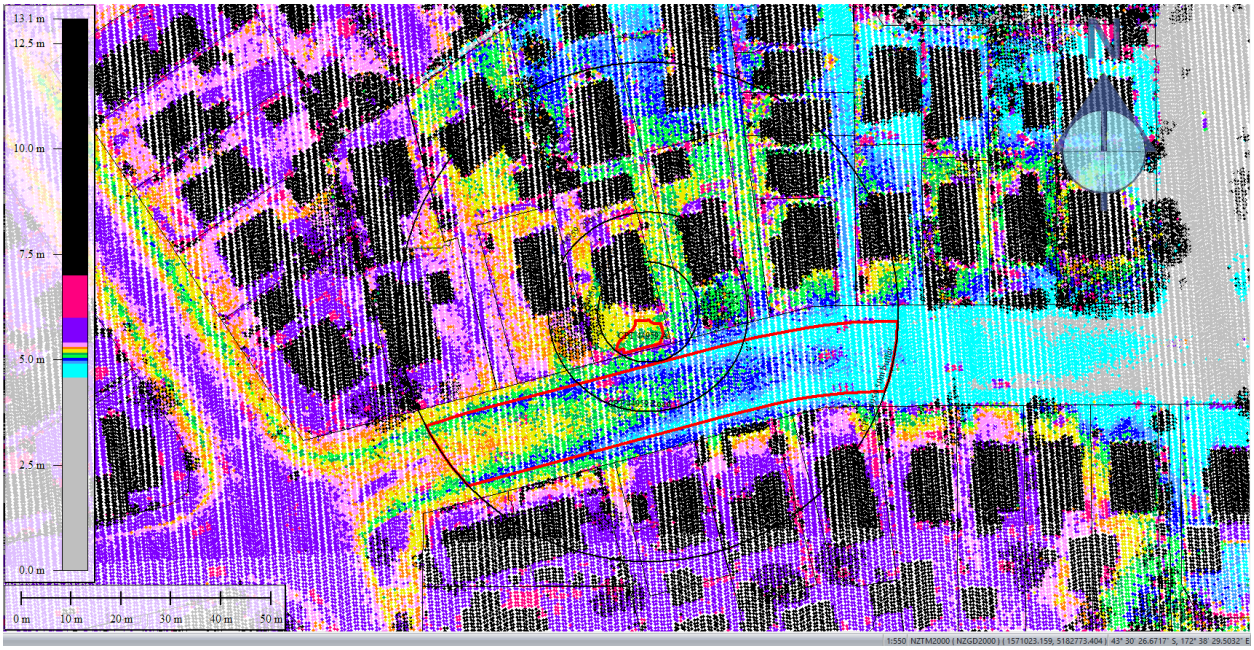

Figure 49: Sep 2011 LiDAR survey.

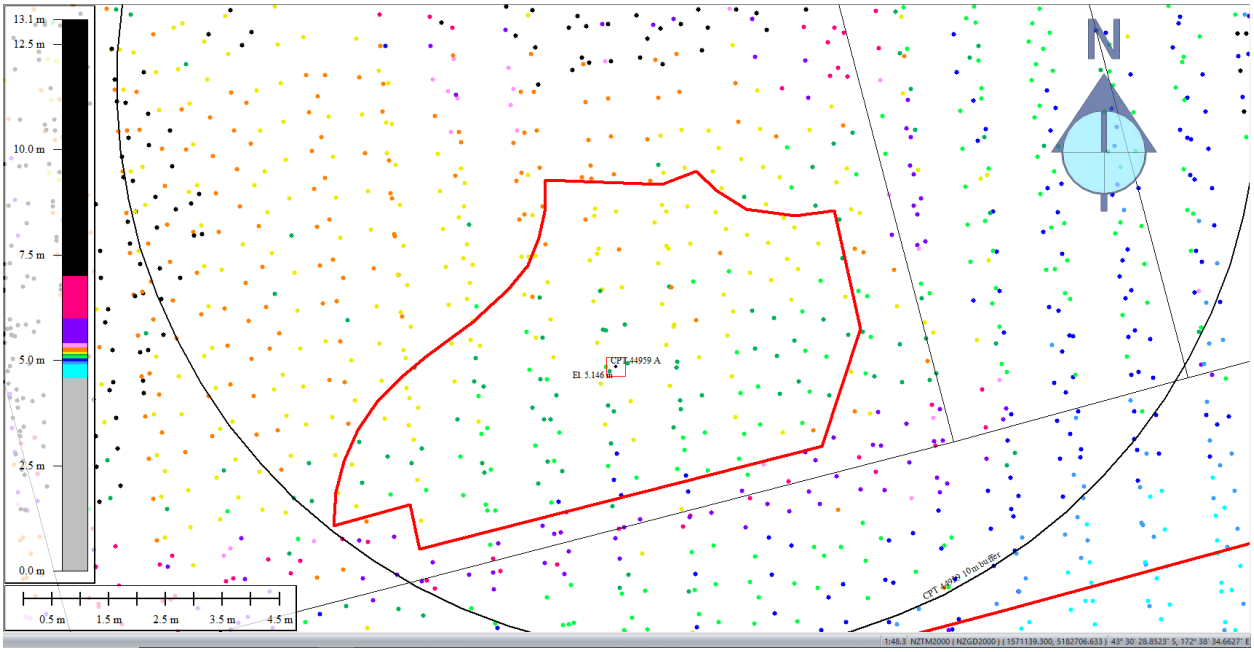

Figure 50: Ground surface elevation averaged over Patch A for Sep 2011 LiDAR survey.

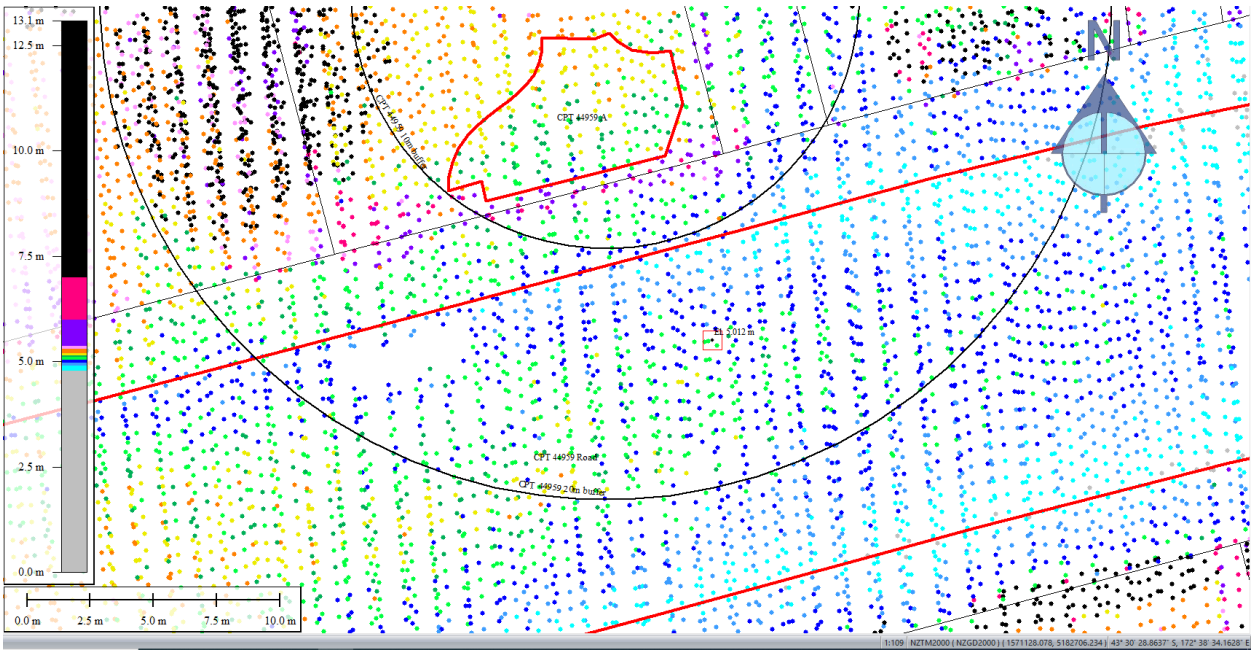

Figure 51: Ground surface elevation averaged over the 20-m buffer for Road for Sep 2011 LiDAR survey.

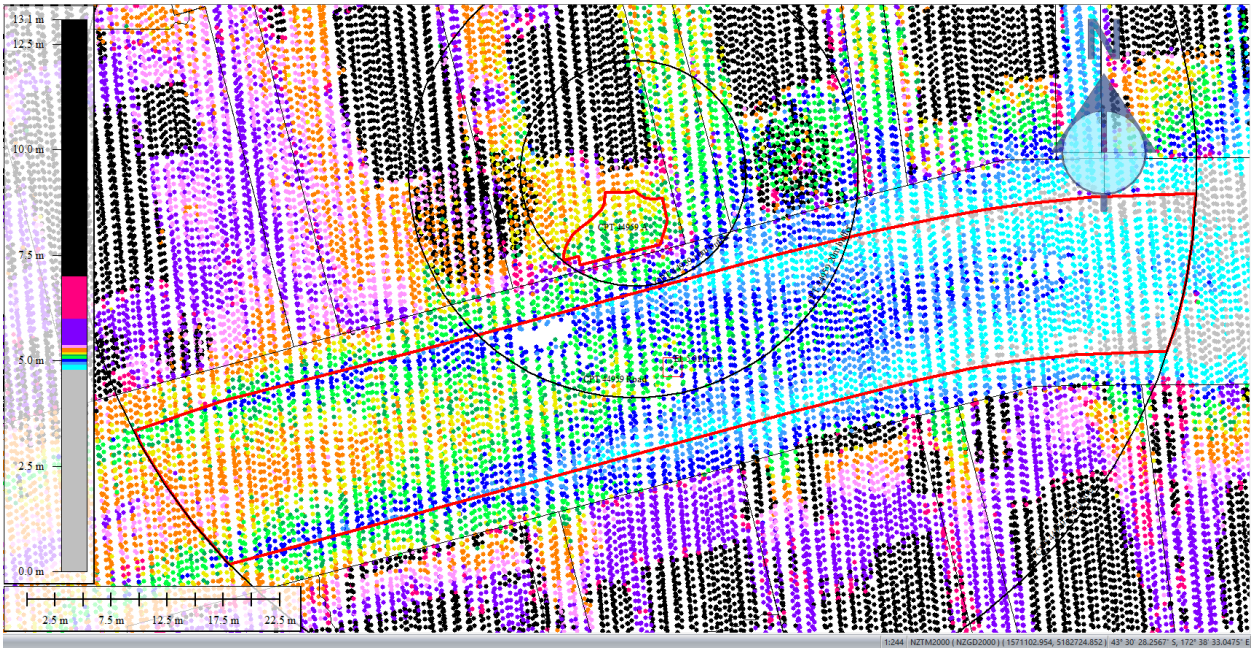

Figure 52: Ground surface elevation averaged over the 50-m buffer for Road for Sep 2011 LiDAR survey.

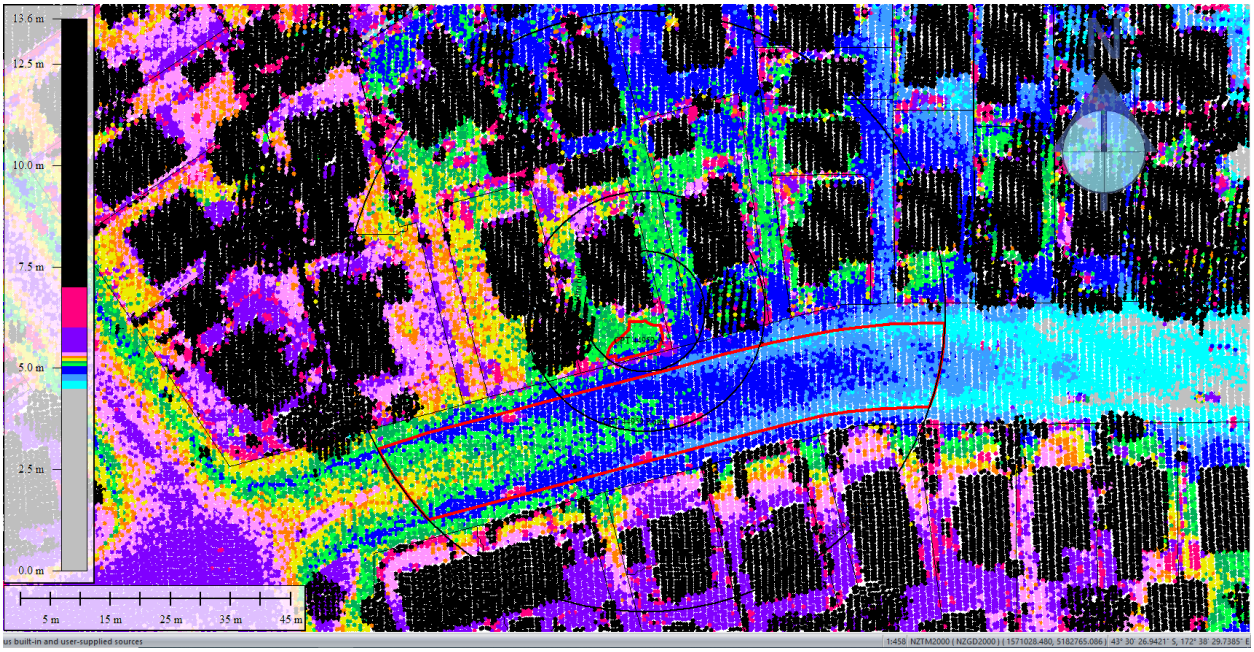

Figure 53: Feb 2012 LiDAR survey.

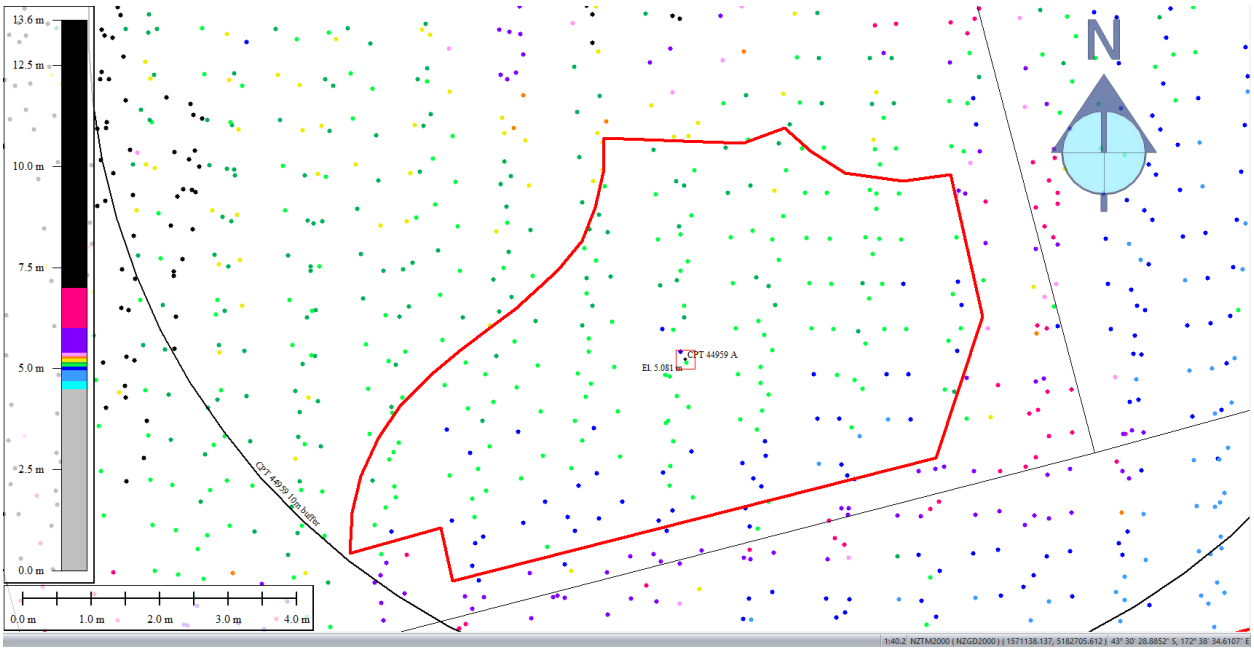

Figure 54: Ground surface elevation averaged over Patch A for Feb 2012 LiDAR survey.

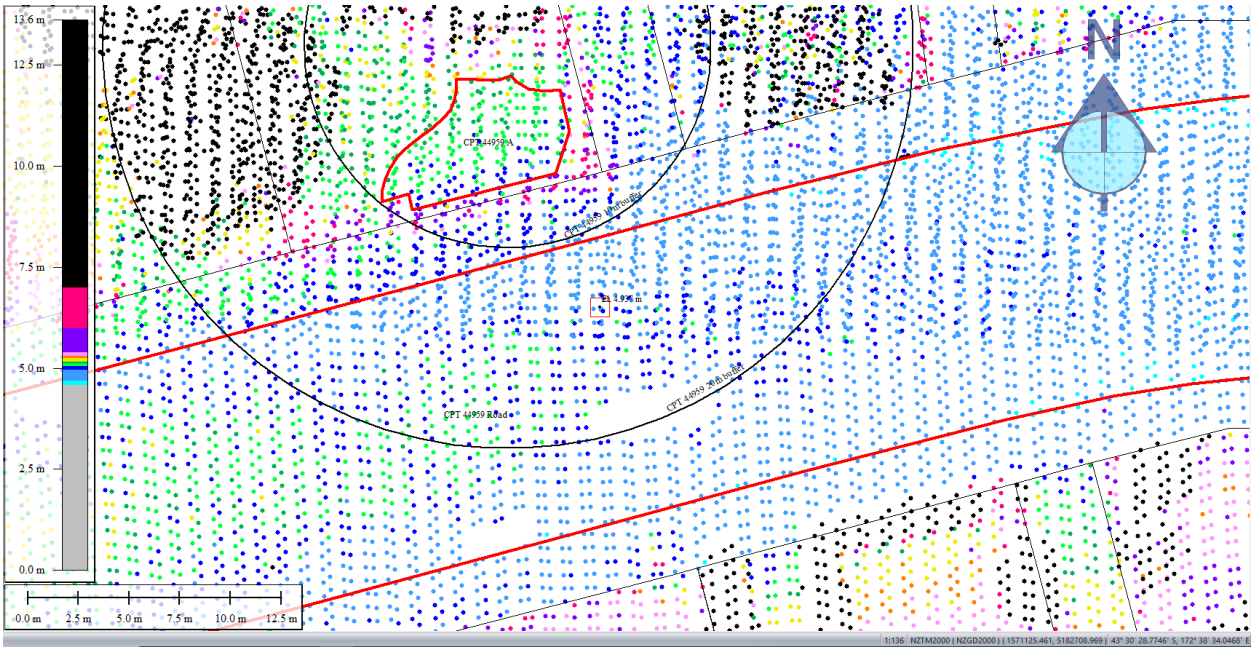

Figure 55: Ground surface elevation averaged over the 20-m buffer for Road for Feb 2012 LiDAR survey.

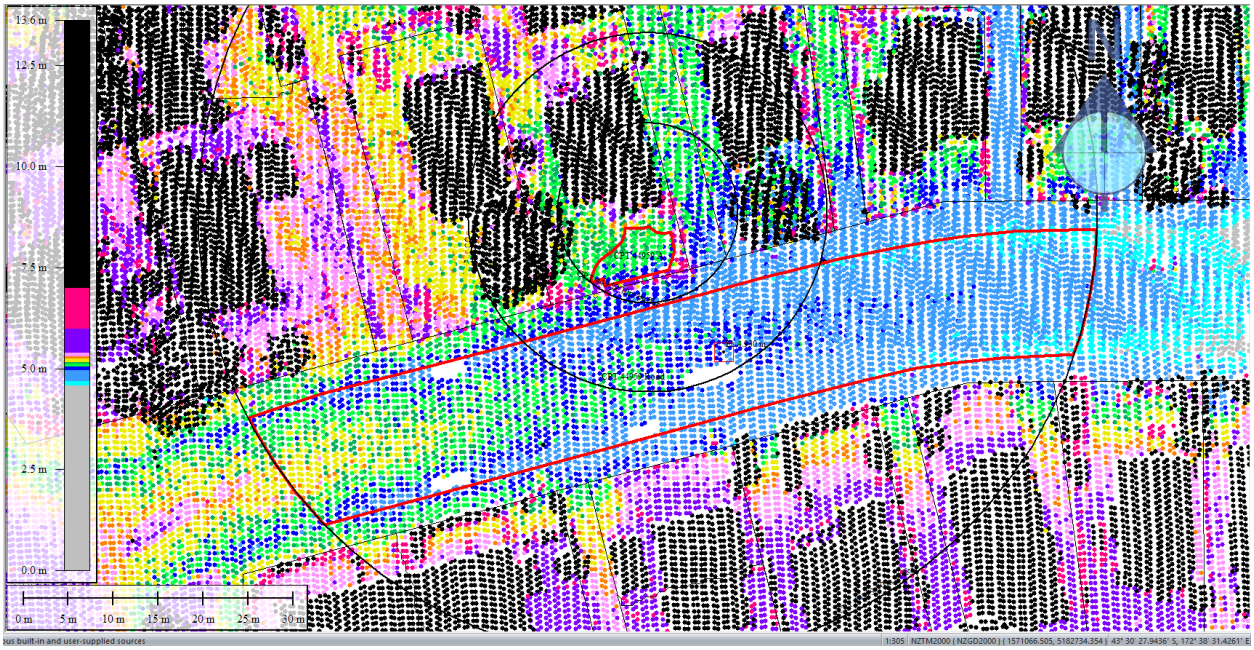

Figure 56: Ground surface elevation averaged over the 50-m buffer for Road for Feb 2012 LiDAR survey.

Figure 57: Oct 2015 LiDAR survey.

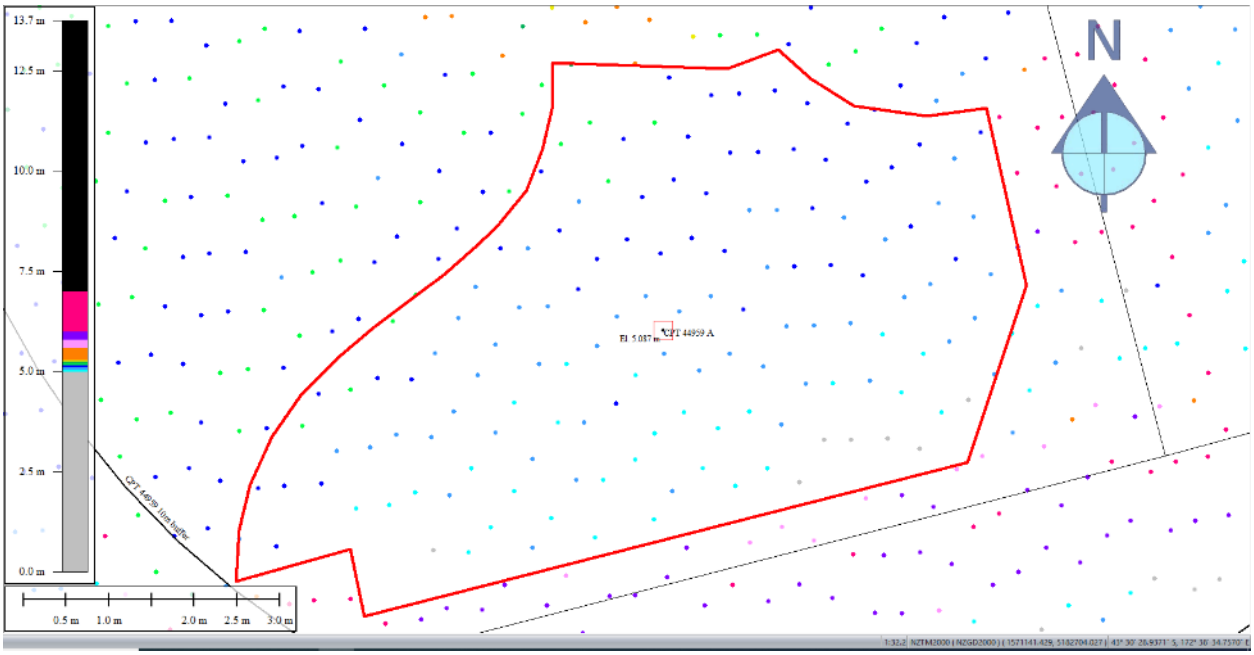

Figure 58: Ground surface elevation averaged over Patch A for Oct 2015 LiDAR survey.

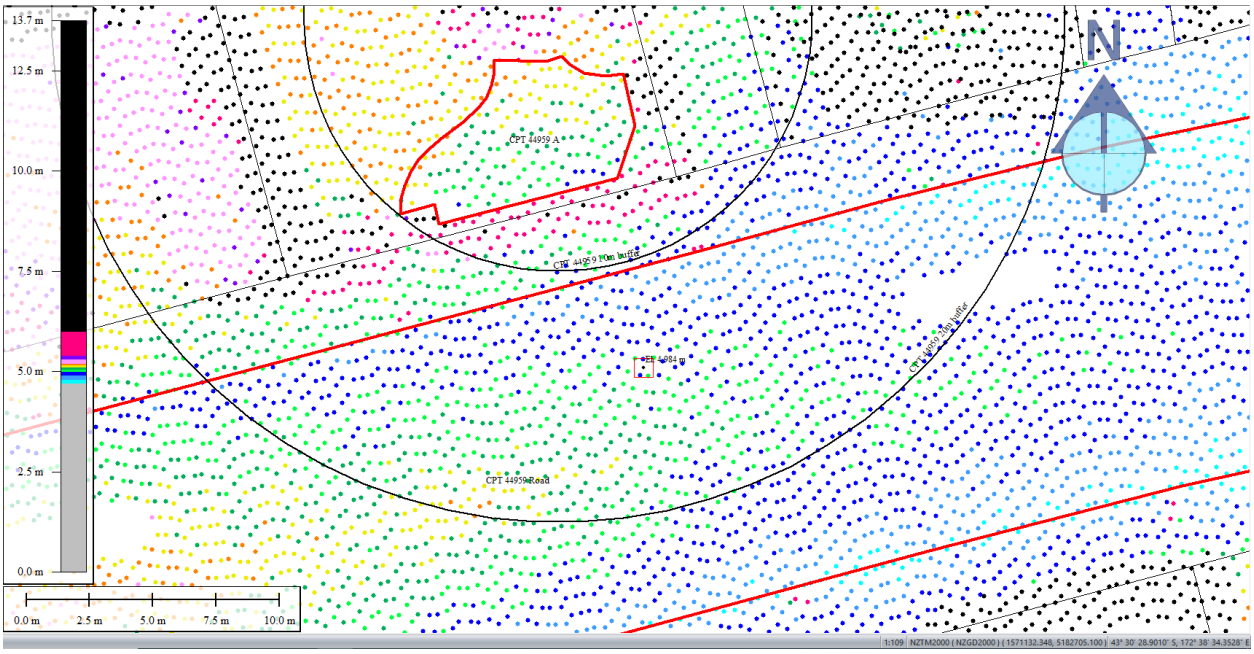

Figure 59: Ground surface elevation averaged over the 20-m buffer for Road for Oct 2015 LiDAR survey.

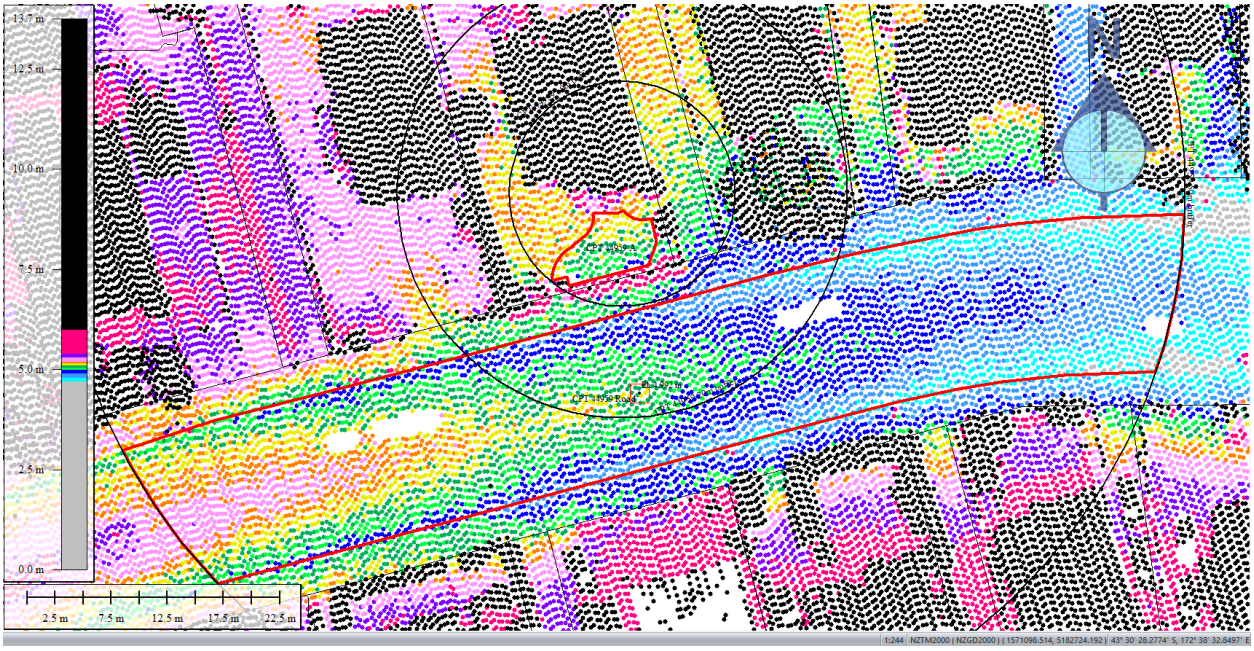

Figure 60: Ground surface elevation averaged over the 50-m buffer for Road for Oct 2015 LiDAR survey.

Figure 61: Ejecta outline for Sep-10 EQ.

Figure 62: Ejecta outline for Feb-11 EQ.

Figure 63: Aerial photograph from 14-15 Jun, 2011.

Figure 64: Ejecta outline for Jun-11 EQ.

Figure 65: Ejecta outline for Dec-11 EQ.

Contents of this figure cannot be shared as doing so is restricted by a Non-Disclosure Agreement.

Figure 66: Some sand was observed in the front garden at the time of inspection in March 2013.

Figure 67: PGA for Sep-10 EQ (st. dev. = 0.300-0.325 ln units).

Figure 68: PGA for Feb-11 EQ (st. dev. = 0.325-0.350 ln units).

Figure 69: PGA for Jun-11 EQ (st. dev. = 0.350-0.375 ln units).

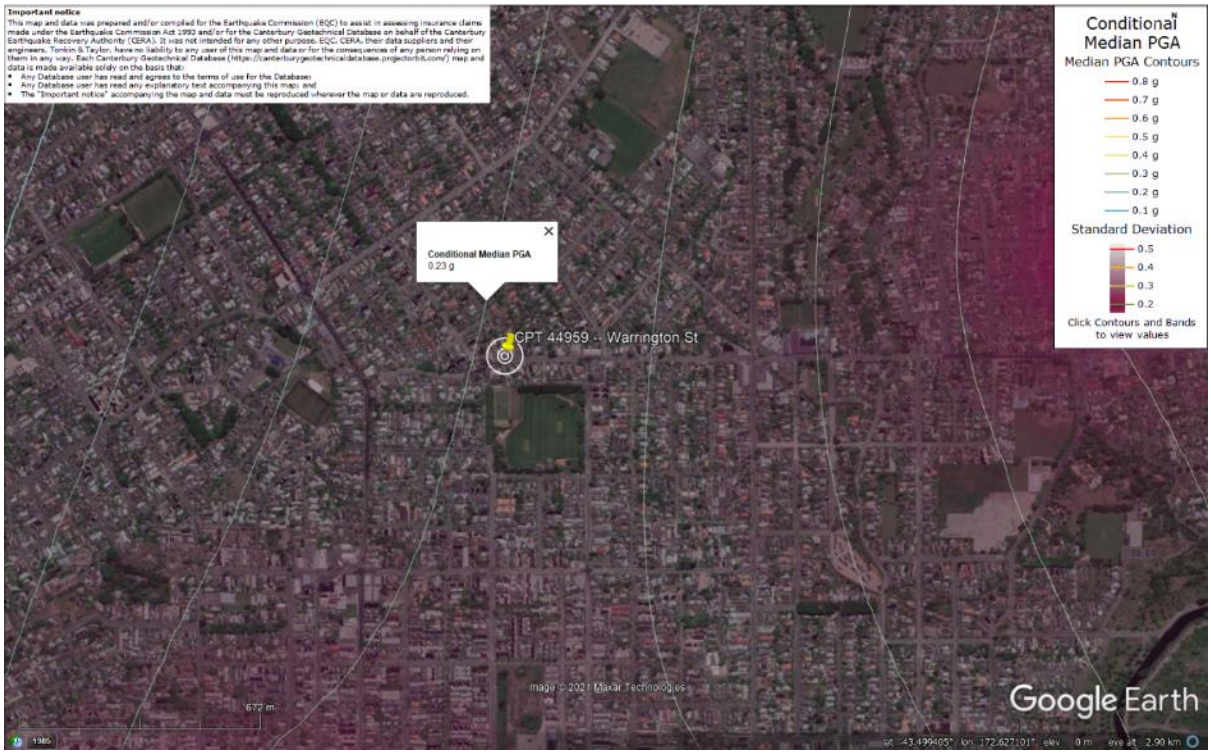

Figure 70: PGA for Dec-11 EQ (st. dev. = 0.350-0.375 ln units).

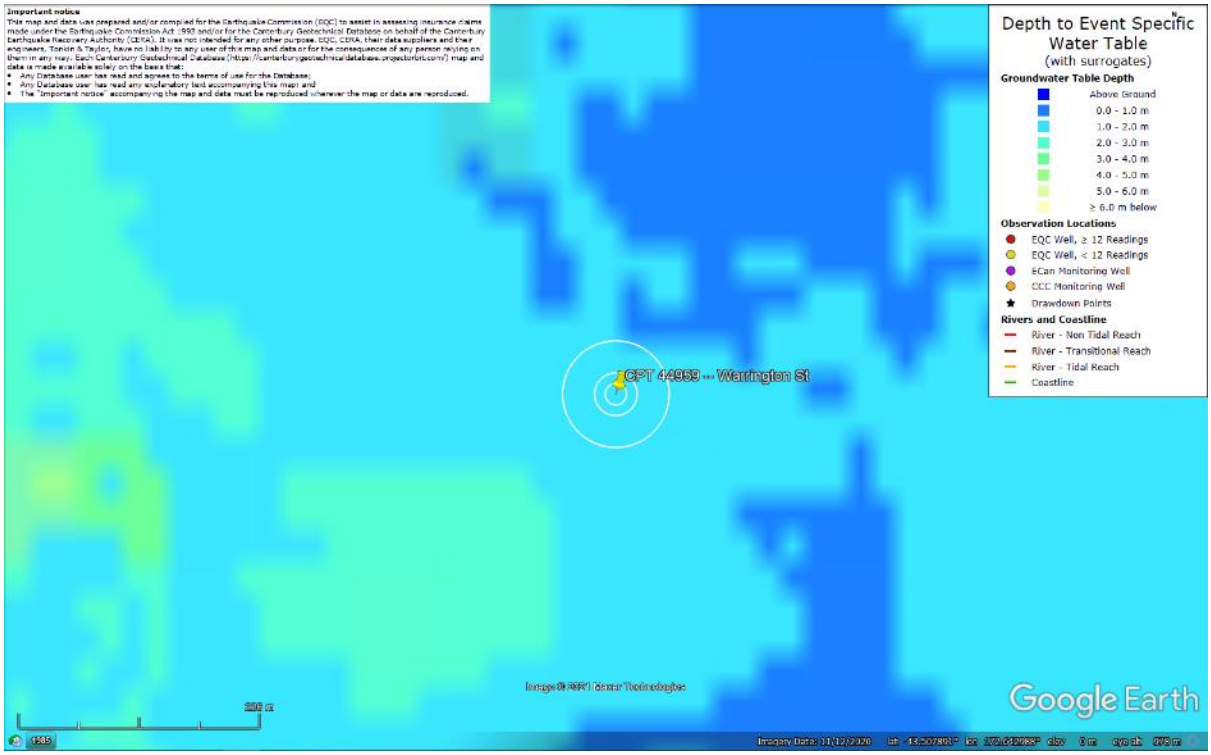

Figure 71: Depth to groundwater table for Sep-10 EQ.

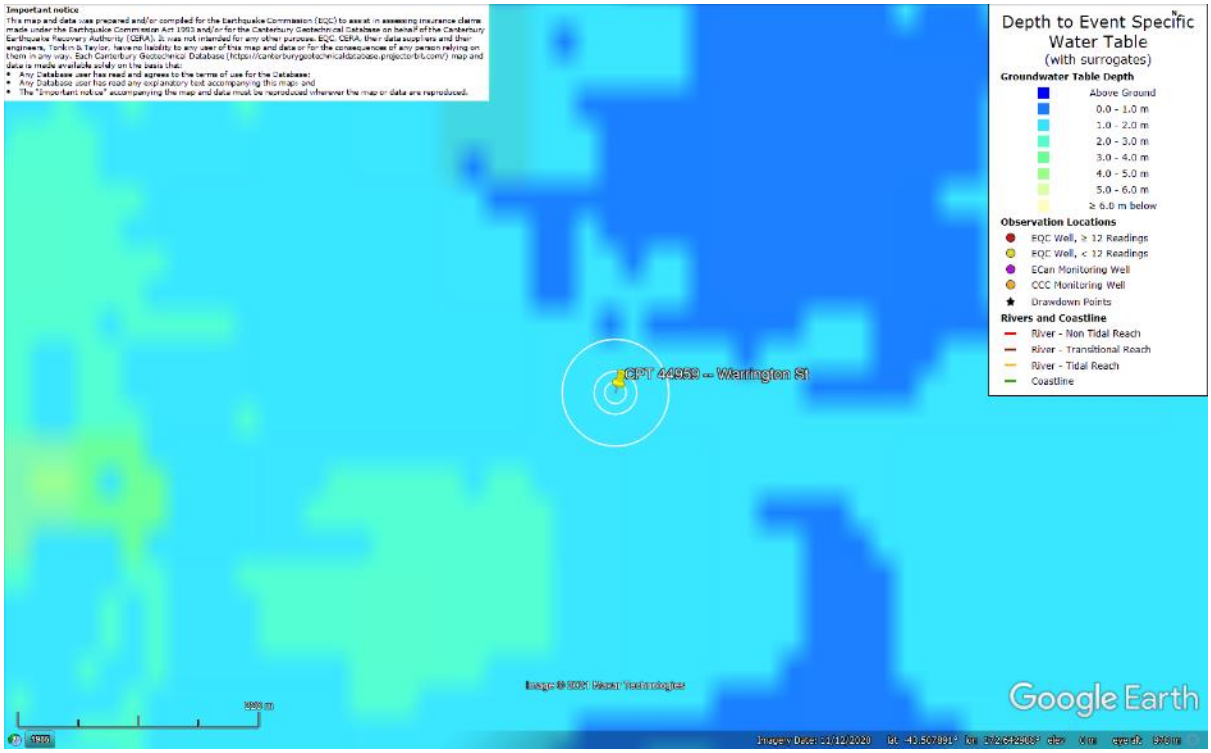

Figure 72: Depth to groundwater table for Feb-11 EQ.

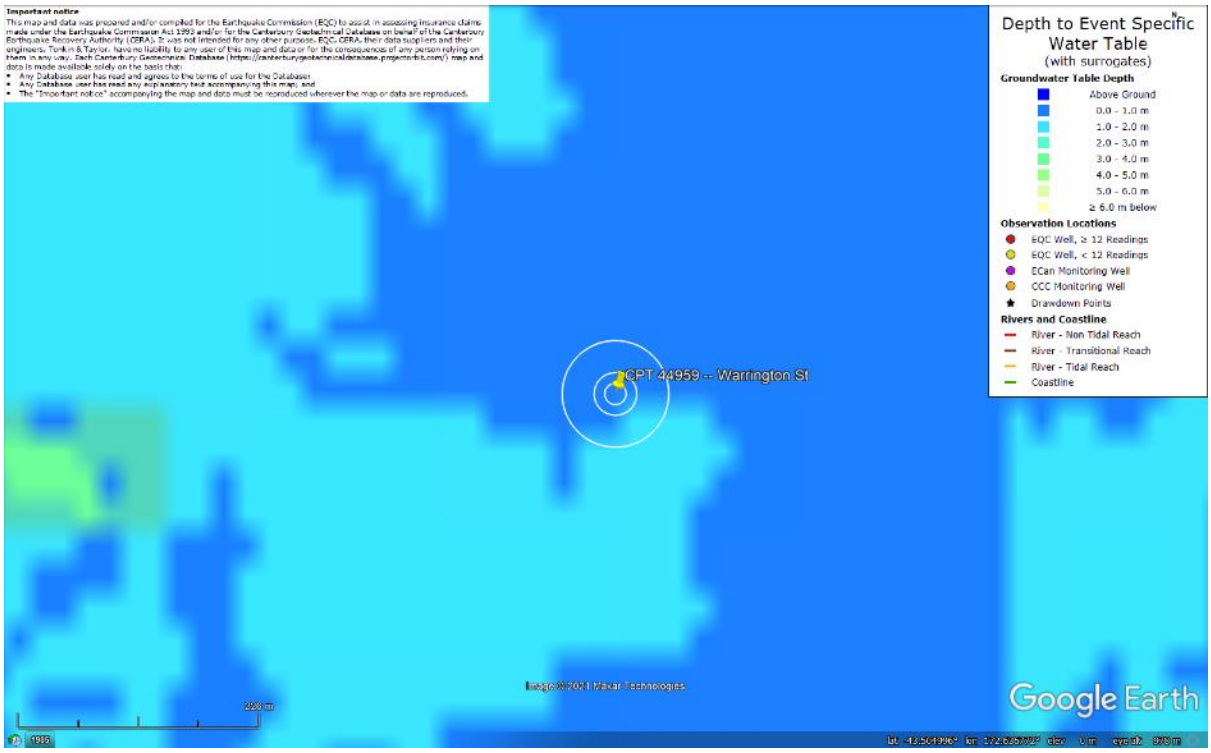

Figure 73: Depth to groundwater table for Jun-11 EQ.

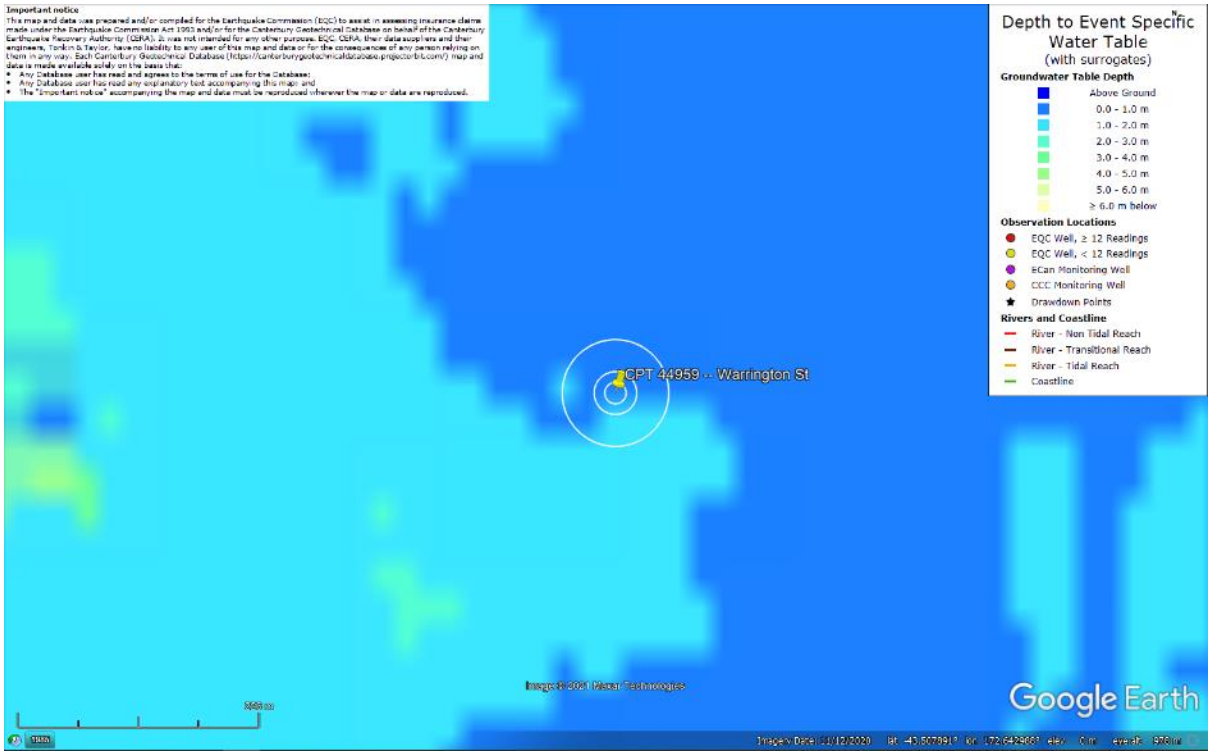

Figure 74: Depth to groundwater table for Dec-11 EQ.

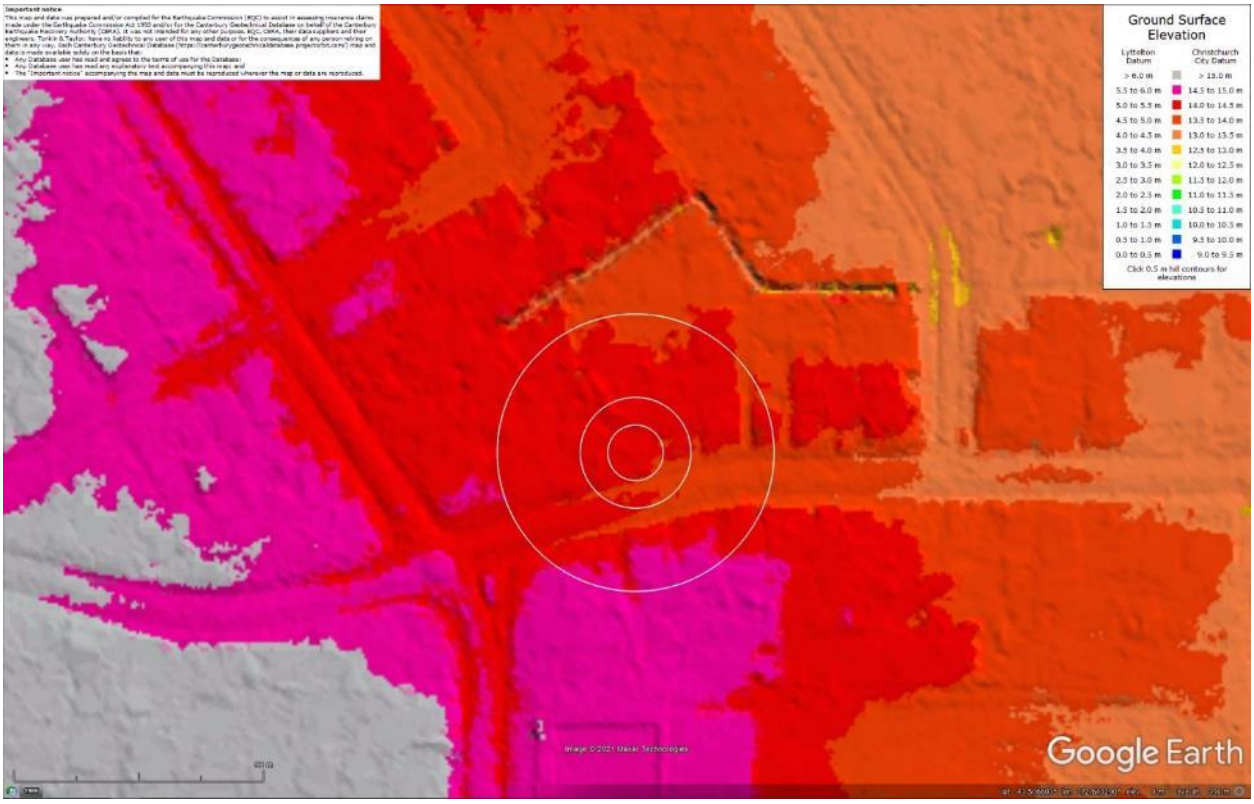

Figure 75: Ground surface elevation according to the Sep-11 LiDAR survey.

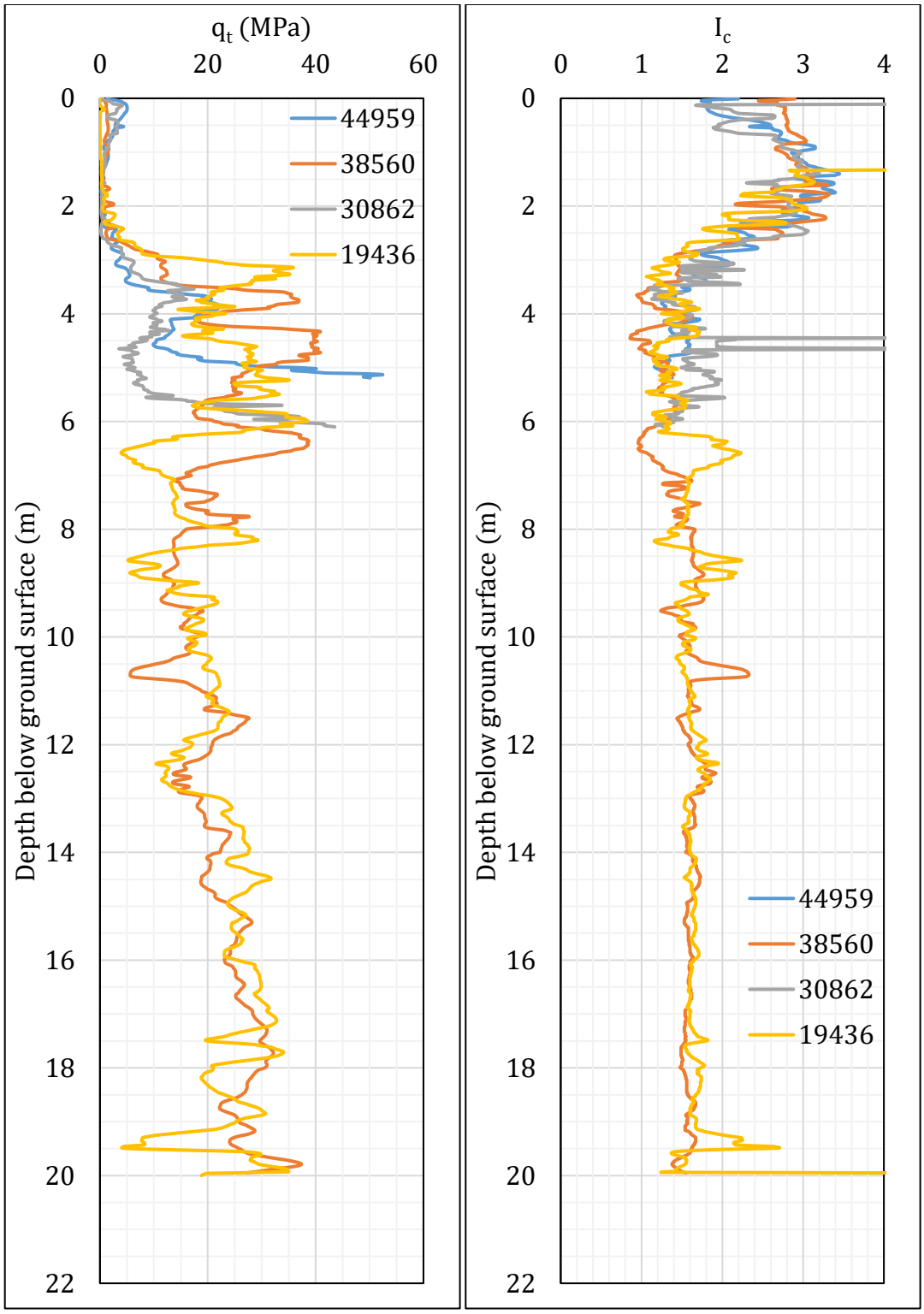

Figure 76: q_t and I_c profiles.

Note 7: The selection of CPTs for the area considered for settlement assessment (Figure 1) is based on the proximity of the CPTs to the considered areas. In accordance with that, the following table shows CPTs that were used for the volumetric settlement analysis in *Cliq v.3.0.3.2*, a CPT soil liquefaction software developed by GeoLogismiki. (The average volumetric settlements were reported in Table 8.)

Table 12: CPT profiles used in volumetric settlement analysis for areas selected for settlement assessment.

CPT ID No.	Patch A	Road
44959	✓	✓
38560		✓
30862		✓
19436		✓

Note: CPT 19436 was used to determine the volumetric settlement for a depth range from 5.2 m to 20 m for CPT 44959 and a depth range from 6.1 m to 20 m for CPT 30862.

Table 13: CPT-based results.

		CPT ID					
EQ Event	Parameter	44959	38560	30862	19436	$\Delta_{5.2m-20m}$*	$\Delta_{6.1m-20m}$*
Sep-10	S_{V1D} (mm)	8	2	20	9	2	2
	LSN	3	1	6	3	1	1
	LPI	0	0	1	0	0	0
	LPI_{ish}	0	0	1	0	--	--
	$D_{FS<1}$ (m)	undet.	undet.	4.79	undet.	--	--
Feb-11	S_{V1D} (mm)	28	14	32	38	18	18
	LSN	10	3	10	10	2	2
	LPI	3	1	4	3	1	1
	LPI_{ish}	3	1	3	1	--	--
	$D_{FS<1}$ (m)	2.40	10.56	2.60	undet.	--	--
Jun-11	S_{V1D} (mm)	16	3	26	14	1	1
	LSN	6	1	9	6	0	0
	LPI	1	0	2	1	0	0
	LPI_{ish}	0	0	1	1	--	--
	$D_{FS<1}$ (m)	3.03	undet.	2.60	undet.	--	--
Dec-11	S_{V1D} (mm)	20	5	28	19	3	3
	LSN	7	2	9	7	1	1
	LPI	1	0	3	1	0	0
	LPI_{ish}	2	0	2	2	--	--
	$D_{FS<1}$ (m)	2.40	undet.	2.60	2.35	--	--

Notes: $D_{FS<1}$ = Depth to the first liquefiable layer ($FS_L<1$) that is at least 200-mm thick, as determined by the Boulanger and Idriss (2016) liquefaction-triggering procedure (P_L=50%, C_{FC}=0.13, and $I_{c,cutoff}$ =2.6), and exported from *Cliq v.3.0.3.2*; undet. = the specified soil layer was not detected; * indicates the amount of S_{V1D}, LSN, and LPI to be added to CPTs 44959 and 30862 due to their penetration depths ending at 5.2 m and 6.1 m, respectively, instead of 20 m.

Note 8: Based on the borehole log (BH 18343, Figure 1), the groundwater table is at a depth of 1.5 m below the ground surface. The soil profile consists of (1) fine to medium sand, SP, the Yaldhurst member of the Springston formation, to a depth of 1.5 m, (2) silt, ML, the Yaldhurst member of the Springston formation, to a depth of 3.45 m, (3) sandy fine to coarse gravel, GW, the Yaldhurst member of the Springston formation, to a depth of 6.7 m, (4) fine to medium sand, SP, the Yaldhurst member of the Springston formation, to a depth of 8.0 m, (5) sandy fine to coarse gravel, GW, the Yaldhurst member of the Springston formation, to a depth of 9.0 m, (6) fine to medium sand, SP, of the Christchurch formation to a depth of 20 m.

Note 9: The ejecta-induced free-field settlement provided in Table 11 is an areal average settlement due to ejecta, which is based on the total settlement assessment area, A_T (provided in Table 9 and repeated in Table 14). However, the considered area was not always covered completely with ejecta; thus, it is important to provide the localized ejecta-induced settlement, too. The localized settlement due to ejecta is estimated using photographic evidence only as

$$S_{E,P\_localized} = \frac{V_E}{A_E}$$

where V_E is the total volume of ejecta within A_T and A_E is the total coverage area of ejecta within A_T. Please note that the areal ejecta-induced settlement provided in Table 14 as S_{E,P_areal} is the same as $S_{E,P}$ in Table 11, which was estimated as

$$S_{E,P\_areal} = S_{E,P} = \frac{V_E}{A_T}$$

where V_E is the total volume of ejecta within A_T and A_T is the total settlement assessment area.

Table 14a: Areal and localized ejecta-induced settlement estimates for Patch A (10-, 20-, and 50-m buffers) based on photographic evidence.

Earthquake Event	A_T (m^2)	A_E (m^2)	V_E (m^3)	S_{E,P_areal} (mm)	$S_{E,P\_localized}$ (mm)
Sep-10	37.7	0	0	0	0
Feb-11	37.7	34.8	1.2-1.8	40±10	45±10
Jun-11	37.7	NA	NA	NA	NA
Dec-11	37.7	0	0	0	0

Notes: S_{E,P_areal} = $S_{E,P}$ reported in Table 11 = areal ejecta-induced settlement; $S_{E,P\_localized}$ = localized ejecta-induced settlement; A_T = total settlement assessment area; V_E = total volume of ejecta within A_T; A_E = total area of ejecta within A_T; The estimates of both areal and localized ejecta-induced settlement are rounded to the nearest 5; Final plus/minus values are also rounded to the nearest 5; NA = Not available.

Table 14b: Areal and localized ejecta-induced settlement estimates for Road (50-m buffer) based on photographic evidence.

Earthquake Event	A_T (m^2)	A_E (m^2)	V_E (m^3)	S_{E,P_areal} (mm)	$S_{E,P\_localized}$ (mm)
Sep-10	1222	847	2.4-4.8	5±5	5±5
Feb-11	1166	1166	15.4-20.0	15±5	15±5
Jun-11	1165	1165	7.5-10.6	10±5	10±5
Dec-11	1271	56.1	0.2-0.4	<5	5±5

Notes: S_{E,P_areal} = $S_{E,P}$ reported in Table 11 = areal ejecta-induced settlement; $S_{E,P\_localized}$ = localized ejecta-induced settlement; A_T = total settlement assessment area; V_E = total volume of ejecta within A_T; A_E = total area of ejecta within A_T; The estimates of both areal and localized ejecta-induced settlement are rounded to the nearest 5; Final plus/minus values are also rounded to the nearest 5.

Summary 2:

- **The best estimate of the localized ejecta-induced free-field ground settlement at the Warrington St site for the SEP 2010, FEB 2011, and DEC 2011 earthquake is 0 mm, 45±10 mm, and 0 mm, respectively. The localized ejecta-induced free-field ground settlement could not be estimated for the JUN 2011 earthquake.**
- **The best estimate of the localized ejecta-induced settlement of the road at the Warrington St site for the SEP 2010, FEB 2011, JUN 2011, and DEC 2011 earthquake is 5±5 mm, 15±5 mm, 10±5 mm, and 5±5 mm, respectively.**